

Determining the Impact of Personal Mobility Carbon Allowance Schemes in Transportation Networks

H. M. Abdul Aziz¹ · Satish V. Ukkusuri²  ·
Xianyuan Zhan²

© Springer Science+Business Media New York 2016

Abstract Personal mobility carbon allowance (PMCA) schemes are designed to reduce carbon consumption from transportation networks. PMCA schemes influence the travel decision process of users and accordingly impact the system metrics including travel time and greenhouse gas (GHG) emissions. We develop a multi-user class dynamic user equilibrium model to evaluate the transportation system performance when PMCA scheme is implemented. The results using Sioux-Falls test network indicate that PMCA schemes can achieve the emissions reduction goals for transportation networks. Further, users characterized by high value of travel time are found to be less sensitive to carbon budget in the context of work trips. Results also show that PMCA scheme can lead to higher emissions for a path compared with the case without PMCA because of flow redistribution. The developed network equilibrium model

This work has been initiated and completed at Purdue University, West Lafayette when the first author was completing his graduate studies. This work does not represent any view of Oak Ridge National Laboratory managed by UT-Battelle for the Department of Energy. This work did not have any kind of financial support from the Oak Ridge National Laboratory managed by UT-Battelle for the department of Energy

✉ Satish V. Ukkusuri
sukkusur@purdue.edu

H. M. Abdul Aziz
aziz.husain.nexus@gmail.com; azizh@ornl.gov

Xianyuan Zhan
zhanxianyuan@purdue.edu

¹ Computational Sciences and Engineering Division, Oak Ridge National Laboratory, 1 Bethel Valley Road, Oak Ridge, TN 37830, USA

² Lyles School of Civil Engineering, Purdue University, West Lafayette, IN, 47907, USA

allows to examine the change in system states at different carbon allocation levels and to design parameters of PMCA schemes accounting for population heterogeneity.

Keywords Low carbon transportation · Carbon reduction goals · Dynamic user equilibrium · GHG emissions · Personal mobility carbon credits

1 Background and motivation

City leaderships across the globe are striving to reach the target level of greenhouse gas (GHG) emissions and energy consumption through strategies that include promoting electric vehicles, energy efficient appliances, energy efficient transportation systems, minimizing building energy consumptions, coordinating smart grid with renewable energy sources, and so on. Minimizing GHG emissions and fuel consumption from road transportation sector is particularly of interest because of its significant contribution (EIA (2014) Annual Energy Outlook 2014) to GHG emissions (about 27 %) and carbon-based fuel consumption (about 28 %). Besides the advancements in engine and fuel technologies, behavioral policies can play a significant role to reduce GHG emissions and achieve the desired low carbon living goals in cities. Personal Carbon Allowance (PCA) schemes are a class of energy policies that are designed based on incentives that influence energy behavior patterns at household level (Fleming and Chamberlin 2011; Fawcett 2010) including building and travel related energy consumptions.

In our previous work (Aziz et al. 2015), we proposed and analyzed a carbon allowance scheme, namely the personal mobility carbon allowance (PMCA) scheme that deals with the daily travel activities at the household level. The travel behavior data were collected through a carefully designed experimental game and econometric models were estimated to understand how an individual makes travel decisions under PMCA scheme. This research focuses on the impact of PMCA at network level. Users in a transportation network will exhibit heterogeneity in terms of travel decisions under PMCA scheme. As a result, the traffic state for a transportation network will evolve because the generalized cost functions for multi-user groups will lead to a distinct dynamic equilibrium condition capturing both travel and carbon cost.

Figure 1 provides a general overview of the PMCA scheme. A regulatory authority such as city leadership determines the total allowable carbon consumption for a system defined with geographical and temporal boundaries. The total allowable consumption is converted into carbon units and allocated among the users in the system. The users spend the carbon credits based on their travel needs. The credits are charged based on the carbon rating of the fuel accounting for its generation cost. For instance, charging an electric vehicle using grid electricity during day time can cost 0.7 per kWh (Fleming and Chamberlin 2011). Users can sell the surplus units and can buy additional units from an auction-based market. Demand and availability of carbon units determine the unit price in the market.

Travel decisions under PMCA will be affected by the amount of carbon credits to be charged on a trip in addition to travel cost. Further, the PMCA system affects the travel behavior in an entirely different manner due to the existence of carbon market

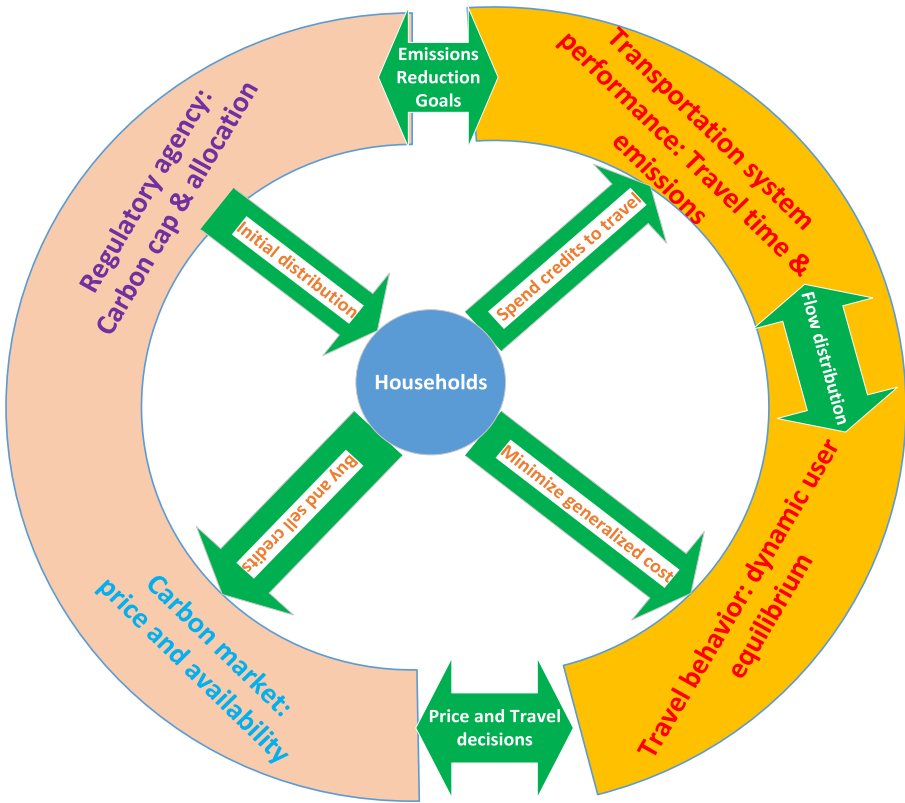


Fig. 1 Personal Mobility Carbon Allowance (PMCA) scheme: carbon budget for daily travel

and initial carbon allocation mechanism. The users have to buy carbon credits from the market with real money in case the initial free quota is diminished. At different conditions describing the price and availability of carbon credits, the decision making process of the users will be different. The remaining budget, market price of the credits, and pro-environmental attitudes are few of the influencing factors. Consideration of carbon cost in addition to travel cost for path and departure time choice will form a new generalized cost function. In Aziz et al. (2015), we estimated the effect of carbon market, initial allocation, and user heterogeneity (in terms of value of travel time and trip purpose) through econometric models using the data from our designed experimental game. The results in (Aziz et al. 2015) provide generalized cost functions specific to trip type and user group categorized based on value of travel time (VOTT).

The objective of this research is to develop a multi-user dynamic equilibrium based network model where each user class has a distinct value of travel time, trip demand, different sensitivity to perceived carbon cost. Figure 2 describes a general framework to analyze the state of transportation network under PMCA scheme. The data through experimental game and estimating generalized cost function are described in

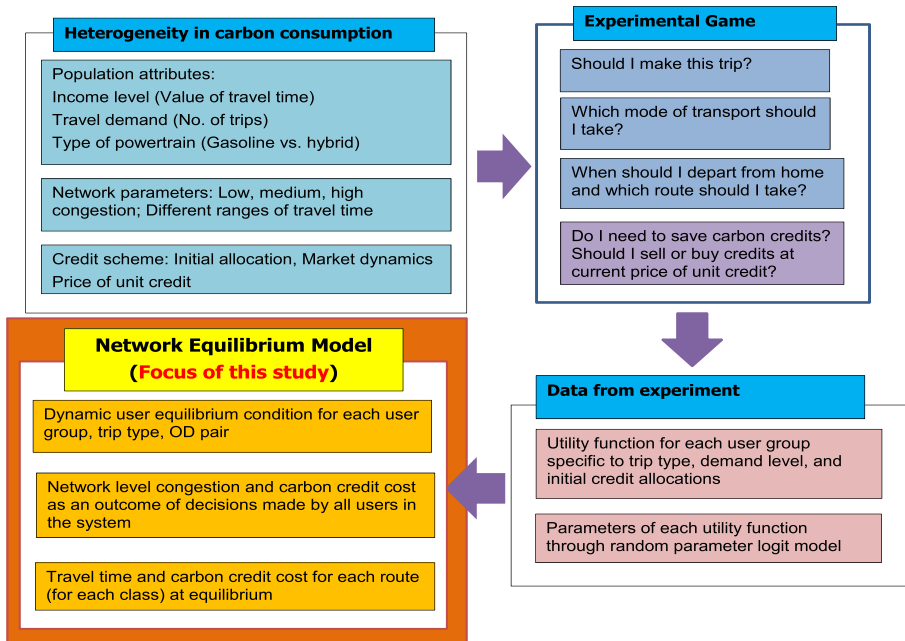


Fig. 2 Generalized framework to network analysis under PMCA scheme. Experimental game and data collection components are described in Aziz et al. (2015)

Aziz et al. (2015). This research focuses primarily on understanding the network-wide impacts due to a PMCA scheme as a result of behavioral adjustments at the household level. To estimate the impacts, a state of the art dynamic network equilibrium model will be developed in this research. The research goals are as follows:

- To develop a multi-class dynamic user equilibrium model accounting the for the travel behavior under personal mobility carbon allowance (PMCA) scheme.
- To explore and investigate the flow redistribution (path level) under the PMCA system accounting for several dimensions of user heterogeneity.
- To examine the change in travel costs and carbon consumption at OD, user class, and path levels under PMCA system at different initial allocations.

2 Related Works and Contributions of this Research

The idea of tradable allowances (or permits) was described in the early works by Coase (1960), Dales (1968), Montgomery (1972), and Verhoef et al. (1997). Tradable allowance systems minimize and equalize the marginal cost of compliance across the entities (agents) without requiring detailed information since the market determines the price (Tietenberg 2003). Cap and trade schemes are a special form of tradable allowance systems with an upper limit on total emissions featuring the ability to trade between the users. The US sulfur dioxide allowance trading system

(Burtraw 2002), the European Union Emission Trading Scheme (EU-ETS), Chicago Climate Exchange, the New England Regional GHG Initiative, Global Warming Solutions Act of 2006 (AB32), and the Kyoto Protocol (Perrels 2010) are some examples that involve upstream players such as manufacturers, regions, nations, and continents.

More recently trading schemes are proposed aiming at the GHG emissions and energy consumptions at household level (Fleming 1997; Hillman and Fawcett 2008; Niemeier et al. 2008). One class of these schemes, namely Personal Carbon Trading (PCT), is recognized by the researchers as an effective instrument to minimize emissions in a cost effective way (Roberts and Thumim 2006; Harwatt et al. 2011). Although debates are still on-going regarding the comparative effectiveness between carbon tax and PCT schemes (Keay-Bright and Fawcett 2005; Raux and Marlot 2005; Starkey 2012b), the unique capabilities to link the end users of energy to the scheme and to accommodate the behavioral aspects of the users make PCT a more attractive scheme (Fleming and Chamberlin 2011; Starkey and Anderson 2005; Fawcett and Parag 2010). Two key concerns related to PCT schemes are: initial setup cost and public acceptability (Starkey 2012b; DEFRA 2008; Howell 2012). A critical review of PCT schemes indicates cost feasibility, higher public *adaptability* leading to *acceptability* over time, and higher level of equity compared with alternative taxation policies (Fawcett 2010, 2012; Connection TLE 2009; Parag and Strickland 2010).

Initial allowance of carbon credits and the equity associated with the distribution stoked the interests among the researchers (Eyre 2010; Fawcett and Parag 2010; Starkey 2008). Most of the studies proposed per capita equal allowance and some provide special distributions to account for the children (Fleming 1997; Bottrill 2006). Arguments can be given against (Starkey 2012a) and for Fleming and Chamberlin (2011), Fawcett (2012), Dresner and Ekins (2004), and Thumim and White (2008) per capita initial distribution. Due to limited number of studies and lack of experimental data, it is not conclusive whether initial per capita distribution is the most equitable way to allocate initial allowances. Again, this is not the key goal of the proposed work. Our model assumes equal allowances for each user in the transportation network.

A group of schemes focus exclusively on reducing GHG emissions and energy consumption from personal travel (Raux and Marlot 2005; Grayling and Gibbs 2006; Keppens and Vereeck 2003; Wadud 2011; Kitthamkesorn et al. 2016). The scope of most of these studies are limited to aggregate level analysis of behavioral change and they do not capture the changes in travel decisions or patterns at household or individual level. Additionally, the data used are obtained in the form of either opinions or responses from questionnaire-based surveys (Capstick and Lewis 2010; Fawcett and Parag 2010; Bristow et al. 2010).

Further, mobility trading schemes are rigorously analyzed as an alternative to tolls on road links (Nagurney and Zhang 2001; Yang and Wang 2011; Nie and Yin 2013; Nie 2012). These studies provide insights on the resulting state of the transportation systems in terms of flow distribution and travel time. In most cases, the focus is not on emissions or energy consumption. Only exceptions are the works by Yin and Lawphongpanich (2006) and Chen and Yang (2012) that apply marginal cost pricing technique to determine the externalities from emissions and by Aziz and

Ukkusuri (2013) that provides a tradable emissions credit scheme for transportation network. In addition network level models with environmental considerations exist (Lin et al. 2016a; Mascia et al. 2016; Lin et al. 2016b; Aziz and Ukkusuri 2012). These approaches are conceptually different from the PMCA scheme and do not incorporate the market behavior into generalized cost function.

2.1 Contributions

This research offers novelty in several ways and addresses limitations of previous works. **First**, unlike qualitative analysis in Wadud (2011), Bristow et al. (2010), and Fawcett and Parag (2010) we provide a rigorous quantitative model accounting for the auction market mechanism obtained from experimental games (Aziz et al. 2015). The generalized cost function directly reflects the travel behavior and activities in the auction market within the designed experiment (see Section 4.4). **Second**, the developed model allows analysis of multiple days and each day with multiple DUE episodes (Section 4.7). Also, the generalized cost function explicitly considers the effect of PMCA and budgeting behavior of households at a disaggregate level considering the heterogeneity both in auction market and daily travel decisions. **Third**, PMCA is conceptually different from mobility credit schemes (Yang and Wang 2011; Nie and Yin 2013; Nie 2012) where the price of unit credit is endogenously computed from the model and this follows the theme of marginal cost pricing (Hearn and Ramana 1998; Aziz and Ukkusuri 2013). This research considers the explicit impact of the auction market and the effect is incorporated exogenously in the generalized cost function which is estimated directly from the data (Aziz et al. 2015). The framework (see Fig. 2) integrates the decision making process at household level and the impact on the system at network level in terms of congestion and emissions accounting for heterogeneity at originating from the dynamics of carbon trading. Finally, this is one of the first network equilibrium models capturing the impacts of carbon allowance scheme at the household level.

3 Multi-Class Characterization

This study considers user heterogeneity based on income level, trip demand, and driving patterns. The value of travel time (VOTT) is often used an indirect measure for income level (Yang and Huang 2004; Yang and Bell 1998; Verhoef and Small 2004; Kockelman and Kalmanje 2005). Further, carbon consumption through fuels are directly influenced by the driving patterns of the users on the road. Generally, higher fluctuation in the speed profile leads to higher emissions in traffic networks (Ahn et al. 2002; Barth and Boriboonsomsin 2008). Finally, emissions (accordingly the carbon consumption) from on-road vehicles depend on the congestion state of the network. The congestion state of a traffic network is highly dominated by the travel choices (Ahn and Rakha 2008) by the users (e.g., route and departure time choice) of the network. The emissions in a highly congested network is significantly different from that of a non-congested network. Modeling the effect of congestion on carbon credit cost and its impact on route and departure time choice behavior

is central in this research and we have a detailed discussion in the methodology section. Also, the travel decisions are impacted by trip purpose, length of the trip, and time-of-the-day.

The travel decision of a user also depends on the remaining carbon credits in her quota at that particular point of time. Additional carbon credits are added at the end of the week as per PMCA system. A traveler with higher credits (with a predefined budget for personal travel and household energy consumption) is more likely to have less sensitivity for emissions (i.e., carbon credit spending) at the end of a week. Based on this attributes mentioned above we define each user class based on five attributes:(a) value of travel time (VOTT), (b) purpose of trip making (e.g., work vs. non-work), (c) available carbon credits prior to making the trip decision, (d) remaining money to spent in the carbon market to buy or sell credits, and (e) value of carbon credits relative to travel time cost. More details are provided in Sections 6.1.1 and 6.1.2.

4 Methodology

The next few sections provide details on the key components of the model that include: the network loading model, travel time estimation, quantification of CO₂ emissions to find carbon credit consumption, characterization of multi-user classes, and the dynamic user equilibrium conditions under PMCA.

4.1 Dynamic Network Loading Under PMCA Scheme

Our formulation embeds a spatial queue based traffic flow model, namely the cell transmission model(CTM), that computes the travel cost and carbon credit cost for the paths in the network. The cell transmission model is originally proposed by Daganzo (1994) and Daganzo (1995). However many variants of the model exist in the literature (Szeto 2013; Carey et al. 2015; Nezamuddin and Boyles 2015) and CTM is widely used as dynamic network loading models. This research follows the models by Han et al. (2011) and Ukkusuri et al. (2012). The unique attributes of our model are as follows:

- (i) Generalized cost structure to capture PMCA attributes. Carbon credit cost is considered in addition to travel cost.
- (ii) Heterogeneity in the population: value of time, value of carbon, and carbon credit market attributes such as unit price of carbon credit and credit availability. This leads to dynamic equilibrium model for multi-user groups.
- (iii) DUE formulation with coupled carbon-cap constraint reflecting the target emissions reduction in the PMCA scheme.

The details of the CTM model along with the initialization, flow propagation, and merging-diverging equations can be found in the Appendix A. The flow propagation equations are extended from the previous work by Ukkusuri et al. (2012) and due to space limitation we do not include them here. The notations and symbols used in this paper are also defined in Appendix A.

4.2 Travel Time Estimation

Travel time computation is a critical element for both DUE formulation. Most of the previous works only compute the travel time without considering schedule delay (Merchant and Nemhauser 1978; Ziliaskopoulos 2000). More recently, the notion of schedule delay is accounted for in the DUE and DSO framework (Ramadurai and Ukkusuri 2007; Han et al. 2011; Ukkusuri et al. 2012). Our proposed model requires the computation of average travel time and we follow the methods by Ramadurai (2009) and Han et al. (2011). Appendix B has the details of travel time estimation.

4.3 Carbon Cost for the Trip

The carbon credit cost to travel in a traffic network is inherently heterogeneous and depends on several attributes pertaining to the vehicle, the user (driver) behavior, traffic conditions, and atmospheric attributes such as humidity, wind speed, temperature profile. Previous researchers (Barth et al. 2004; Barth and Boriboonsomsin 2008) estimated the relationship between average trip speed and CO₂ emissions. The emission on a link can be expressed as polynomials:

$$\psi_e = a_0 + a_1 \times v_p + a_2 \times (v_p)^2 + a_3 \times (v_p)^3 + a_4 \times (v_p)^4 + \dots \quad (1)$$

where, a_j s are the coefficients, v_p is the average trip speed. ψ_e is the total CO₂ emissions for the trip. Relationships also exist for electric vehicles. Based on the data from Tesla Motors, the average CO₂ from EVs is about 12.6 g/km. Gardner et al. (2013) use the following equation to compute the energy requirement from EV:

$$EC_{EV} = 1.79 \times 10^{-8} \times (v)^4 - 4.073 \times 10^{-6} \times (v)^2 + 3.654 \times 10^{-4} \times (v)^2 - 4(v)^4 - 0.0109v + 0.2372$$

The steps to compute carbon cost for a path are as follows:

- *Step 1:* Compute the average travel time $TT_{p,t}$ for the path with departure time t
- *Step 2:* Estimate the average speed $V_{p,t}$ using the trip length l_p
- *Step 3:* Use the appropriate emissions estimation equation based on engine type
- *Step 4:* Convert the emissions into carbon credit using proper factor (e.g., one can assume 100g of CO₂ = 1 carbon credit)

The path level carbon cost can be computed as follows:

$$CC_{p,t} = \alpha_1 v_{p,t}^4 - \alpha_2 v_{p,t}^3 + \alpha_3 v_{p,t}^2 - \alpha_4 v_{p,t} + \alpha_5. \quad (2)$$

$\alpha_1, \alpha_2, \alpha_3, \alpha_4,$ and α_5 are input parameters that depend on type of engine, geographical location, and atmospheric attributes such as wind speed, temperature profile, etc.

$v_{p,t}$: Average speed of the trip when a user departs at time $t \in T_f$ on path p .

$$v_{p,t} = \frac{\sum_{i \in I_p} L_i}{TT_{p,t}} \quad (3)$$

I_p : set of all cell index constituting path p ,

L_i : Length of cell i . Next we describe the generalized cost function and its parameters for each user class.

4.4 Generalized Cost Function Under PMCA

Consider an individual $i \in \mathbb{I} : \{1, \dots, i, \dots, I\}$, with total N trips (set of trips $\mathbb{N} = \{1, \dots, n, \dots, N\}$). For any trip $n \in \mathbb{N}$, an individual chooses travel option \hat{k} from the set of all feasible travel options to make the trip defined as $\mathbb{K} = \{1, \dots, \hat{k}, \dots, \hat{K}\}$. Each travel option has two dimensions: path p and departure time t , and is associated with a cost in carbon credits $CC_{\hat{k}}$ and a travel cost $TC_{\hat{k}}$. The generalized cost function is specific to a user group characterized based on income level, value of travel time, and number of trips made. Further characterization is made based on trip purpose (e.g., work vs. non-work trips), congestion level, and carbon credit allocation in the scheme. Denote, $\Psi_{i,\hat{k}}$ as the generalized cost of travel for an individual i choosing the travel alternative (combination of departure time and path) \hat{k} in one of her trip making instances. For simplicity, we present the formulation for a specific trip purpose, congestion level, initial credit allocation and for a specific user group. The notations that characterize the user group, congestion level, and carbon credit allocation are omitted. For any travel decision instance we observe the following attributes: $TC_{\hat{k}}$: the travel time cost associated with option \hat{k} ,

$CC_{\hat{k}}$: the carbon cost in terms of units of credits associated with option \hat{k} ,

RB_i : remaining carbon credits for individual i prior to making decision,

H_i : available money for individual i to purchase carbon credits from the market.

Incorporating these attributes, the generalized trip cost function, when travel option \hat{k} is chosen, can be written as:

$$\Psi_{i,\hat{k}} = \beta^{TC} TC_{\hat{k}} + \beta^{CC} CC_{\hat{k}} + \beta^{RB} RB_i + \beta^H H_i \tag{4}$$

With data on the travel decisions for all options $\hat{k} \in K$ for all trips, the coefficients $\beta_m^{TC}, \beta_m^{CC}, \beta_m^{RB}, \beta_m^H$ can be estimated for each group $m \in M$. To collect data we designed experiments and have estimated the coefficients using random parameter models (please see the previous chapter). The parameters are estimated specific to each user class and each trip type. The generalized cost $GC_{p,t}^m$ when departing at time $t \in T_e$ on path $p \in P^w$ for OD pair $w \in W$ by a user in group $m \in M$ can be expressed as:

$$GC_{p,t}^m = \beta_m^{TC} TC_{p,t}^m + \beta_m^{CC} CC_{p,t}^m + \beta_m^{RB} RB_m + \beta_m^H H_m \tag{5}$$

Note that, each path is unique, therefore we do not use the OD index w . Also, the remaining carbon budget and money are only specific to the user class and independent of the current travel option (p, t) . Only travel cost is specific to a user class $m \in M$ because the value of travel time and the penalties for early and late arrival at destination is different for each group.

4.5 Dynamic User Equilibrium Condition

The dynamic user equilibrium (DUE) condition for PMCA-DUE specific to a user class is defined as follows:

The generalized cost of each path between an O-D pair is equal and minimum at any departure time interval with non-zero departure rate for the paths.

In other words, at equilibrium there is no incentive for a user belonging to a particular class to switch path and departure time (i.e., travel option). While this definition of network equilibrium is similar to dynamic equilibrium problems in the literature (Ukkusuri et al. 2012; Szeto 2013; Ma et al. 2015), a key difference is that the generalized cost in our case is a function of carbon credit consumption and the accommodation of user heterogeneity in formulation.

For each user class $m \in M$ and OD pair $w \in W$ in the network we have the following dynamic equilibrium condition:

$$\begin{aligned}
 &0 \leq r_{p,t}^m \perp GC_{p,t}^m - GC_w^{m*} \geq 0, \\
 \Rightarrow &0 \leq r_{p,t}^m \perp \beta_m^T TC_{p,t}^m + \beta_m^{CC} CC_{p,t} + \beta_m^{RB} RB_i + \beta_m^H H_i - GC_w^{m*} \geq 0 \quad (6)
 \end{aligned}$$

The travel cost $TC_{p,t}^m$ is computed as follows:

$$TC_{p,t}^m = \alpha_1^m TT_{p,t} + \alpha_2^m e_{p,t} + \alpha_3^m l_{p,t} \quad (7)$$

4.6 Demand Satisfaction Constraints

At equilibrium the departure rate for all paths must accumulate to the demand for the O-D pair.

$$0 \leq GC_w^{m*} \perp \sum_{p \in P_w} \sum_{t=0}^{t_e} r_{p,t}^m - d_w^m \geq 0, \quad \forall w \in W, m \in M \quad (8)$$

This constraint is similar to Han et al. (2011) and Ukkusuri et al. (2012) with the addition of user class level constraint. At equilibrium we have,

$$\sum_{p \in P_w} \sum_{t=0}^{t_e} r_{p,t}^m - d_w^m = 0, \quad \forall w \in W, m \in M \quad (9)$$

The equations that compute $e_{p,t}$ and $l_{p,t}$ can be transformed into equivalent complementarity conditions (see Han et al. (2011)).

4.7 Dynamic User Equilibrium with Personal Mobility Carbon Allowance (DUE-PMCA)

PMCA scheme is continuous in nature. With a choice of interval for the auction it can continue for years. The model presented here assumes a weekly auction format. A user only participates in the auction after a week. The price changes after each week, however the remaining carbon credits and money continue to change as users

make travel decisions during the week. The model divides the time horizon into multiple segments. This segmentation helps to run the model efficiently compared with a single analysis with a very long time horizon (e.g., entire day or week). We refer to such segment as a DUE-episode. For instance, the morning peak hour (6 am to 9 am) is a DUE-episode. DUE-PMCA formulates the model with multiple DUE-episodes as required by the time horizon. For instance, a typical week day can have several DUE-episodes covering all travel activities from the 4 am to 12 midnight. Each DUE-episode is distinct in terms of demand and purpose of the trips. For instance, a DUE-episode for 12 noon-2 pm will have more grocery trips.

Define a finite time horizon $\{1, 2, \dots, \pi, \dots, \Pi\}$ and a set of DUE-episodes for the horizon $\{E_1, E_2, \dots, E_\pi, \dots, E_\Pi\}$. Each episode E_{pi} follows the conditions as described by the Eqs. 6 and 8. Now we introduce a necessary constraint for the DUE-PMCA model that reflects the carbon consumption cap for the system. PMCA schemes are designed to meet targets such as reducing the carbon consumption by 5 % from the base case. To meet this requirement, carbon credits equivalent to 95 % of the base case are distributed among the users. Therefore the model needs to ensure that the total carbon consumption for all episodes should not exceed 95 % of the base consumption.

$$\sum_{E_\pi: \pi \in \{1, \dots, \Pi\}} \left\{ \sum_{t \in T_f} \sum_{m \in M} \sum_{w \in W} \sum_{p \in P^w} CC_{p,t}^m * r_{p,t}^m \right\}_\pi \leq \Theta \tag{10}$$

In Eq. 10, Θ defines the desired threshold for carbon consumption. Equation 10 is a coupling constraint for all the DUE-episodes considered in the model. Now the entire model can be presented as follows:

For each episode E_π :

A1. DUE Condition:

$$0 \leq r_{p,t}^m \perp \beta_m^{TC} TC_{p,t}^m + \beta_m^{CC} CC_{p,t} + \beta_m^{RB} RB_i + \beta_m^H H_i - GC_w^{m*} \geq 0$$

A2. Demand satisfaction:

$$0 \leq GC_w^{m*} \perp \sum_{p \in P_w} \sum_{t=0}^{t_e} r_{p,t}^m - d_w^m \geq 0, \forall w \in W, m \in M$$

A3. Travel time computation (Eq. 39)

A4. Carbon cost computation (Eq. 2)

A5. Non-negativity constraints

Coupling constraint:

B. carbon cap:

$$\sum_{E_{\pi}:\pi \in \{1, \dots, \Pi\}} \left\{ \sum_{t \in T_f} \sum_{m \in M} \sum_{w \in W} \sum_{p \in P^w} C C_{p,t}^m * r_{p,t}^m \right\}_{\pi} \leq \Theta$$

$$\Rightarrow \sum_{\pi=1}^{\Pi} \theta_{\pi} \leq \Theta$$

θ_{π} : Total carbon consumption for an episode π .

4.8 Equivalent VI

For each DUE episode we can write the complementarity formulation in a compact format:

$$0 \leq r_{p,t}^m \perp G C_{p,t}^m - G C_w^{m*} \geq 0 \quad \forall p \in P^w, w \in W, t \in T_e. \quad (11)$$

The demand satisfaction and non-negativity constraints can be represented as follows:

$$\Omega \triangleq \left\{ \sum_{p \in P_w} \sum_{t=0}^{t_e} r_{p,t}^m - d_w^m = 0, \mathbf{r} \geq 0 \quad \forall w \in W, m \in M \right\} \quad (12)$$

Now define the θ as the total carbon consumption for the episode and it should be non-negative. The equivalent VI formulation for a single DUE-episode will be:

$$G C^T (\mathbf{r} - \mathbf{r}^*) \geq 0, \quad \mathbf{r}^* \in \Omega \quad (13)$$

$$0^T (\theta - \theta^*) \geq 0, \quad \theta^* \in \mathbb{R}_+ \quad (14)$$

Now for a PMCA-DUE problem with Π DUE-episodes we can have:

$$\begin{aligned} G C_1^T (\mathbf{r}_1 - \mathbf{r}_1^*) &\geq 0, & \mathbf{r}_1^* &\in \Omega_1, \\ 0^T (\theta_1 - \theta_1^*) &\geq 0, & \theta_1^* &\in \mathbb{R}_+, \\ &\dots & \dots & \\ G C_{\pi}^T (\mathbf{r}_{\pi} - \mathbf{r}_{\pi}^*) &\geq 0, & \mathbf{r}_{\pi}^* &\in \Omega_{\pi}, \\ 0^T (\theta_{\pi} - \theta_{\pi}^*) &\geq 0, & \theta_{\pi}^* &\in \mathbb{R}_+, \\ &\dots & \dots & \\ G C_{\Pi}^T (\mathbf{r}_{\Pi} - \mathbf{r}_{\Pi}^*) &\geq 0, & \mathbf{r}_{\Pi}^* &\in \Omega_{\Pi}, \\ 0^T (\theta_{\Pi} - \theta_{\Pi}^*) &\geq 0, & \theta_{\Pi}^* &\in \mathbb{R}_+, \\ &\sum_{\pi=1}^{\Pi} \theta_{\pi} &\leq \Theta. \end{aligned}$$

Now we denote,

$$\Omega_{\theta} \triangleq \left\{ \sum_{\pi=1}^{\Pi} \theta_{\pi} \leq \Theta \right\} \quad (15)$$

Also define, $Y = [\mathbf{r}_1, \theta_1, \mathbf{r}_2, \theta_2, \dots, \mathbf{r}_{\pi}, \theta_{\pi}, \dots, \mathbf{r}_{\Pi}, \theta_{\Pi}]^T$;
 $C = [G C_1, 0, G C_2, 0, \dots, G C_{\pi}, 0, \dots, G C_{\Pi}, 0]^T$ and

$\Omega : \{\Omega'_1 \times \Omega'_2 \times \dots \times \Omega'_\pi \times \dots \times \Omega'_\Pi \times \Omega_\theta\}$. Now the system of VIs can be represented in a compact format.

$$\mathbf{C}^T (\mathbf{Y} - \mathbf{Y}^*) \geq 0, \quad \mathbf{Y}^* \in \Omega \tag{16}$$

The solution of the $VI(\mathbf{C}, \Omega)$ will be the solution of formulation **AB**

5 Solution Approach

This section describes the solution approaches to solve the DUE-PMCA problem. In the previous section, we have shown that the original problem can be transformed into a variational inequality (VI) problem. This section proposes solution methods for the equivalent VI problem. Challenges associated with the solution technique mostly arise with the nature of the cost function that is non-differentiable, non-convex, and non-monotone. The reason is that we obtain the cost function from the CTM simulation. Commonly used commercial solvers such as KNITRO and PATH are not able to solve this problem for reasonable sized networks. Addressing this issue, this research approaches with derivative-free algorithms, namely the projection algorithm, to solve the equivalent VI problem.

We propose two approaches to solve the problem. The first approach is to use the basic projection algorithm to solve the VI problem with coupling constraints of carbon cap. The second approach is to decompose the original VI problem and solve a series of smaller VI problems where the carbon cap constraints are associated with each individual DUE-episode.

5.1 Basic Projection Method for the Coupled VI

To solve a $VI(F, K)$ we compute a sequence of points $\{u^i\}_{i=1}^\infty$ starting with an initial solution x^0 .

$$u^{i+1} = \Lambda_K[u^i - F(u^i)], \quad \forall i = 1, 2, \dots, \infty \tag{17}$$

$\Lambda_K(u)$ denotes the the projection of u on the feasible region K . In other words, one defines the projection:

$$\varpi = \arg \min \|z - u\|^2 \tag{18}$$

The convergence of the solution requires that F should be monotone. In our case, the cost function does not have this property and direct convergence cannot be shown. However the feasible region that has only systems of linear equations and inequalities is compact. With this compact feasible region it is possible to show sub sequential convergence when the VI problem is solved using projection method. Ukkusuri et al. (2012) has the proof for the case without carbon cap constraint. Since carbon cap constraints are linear in nature and the properties of the feasible region remain the same, the same proof applies for our case.

Algorithm steps:

Data: Initialize with a feasible $\mathbf{Y}^0 \in \Omega$

Step 0: Set $i = 0$.

Step 1: Computation: $CTM(\mathbf{Y}), \mathbf{C}, \mathbf{Y}$

Step 2: Find the projection: $\mathbf{Z}^* = \arg \min_{z \in \Omega} [Z - (\mathbf{Y}^i - \lambda \mathbf{C}(\mathbf{Y}^i))]$.

Step 3: If $\|\mathbf{Z}^* - \mathbf{Y}^i\| < \xi$, Terminate. Else, $\mathbf{Y}^{i+1} = \mathbf{Z}^*$ and Go to Step 1.

Our experience with the basic projection algorithm shows that the algorithm is not efficient to solve large networks and do not meet the error tolerance criterion at most cases. To resolve the issue we propose a decomposed approach where each DUE-episode is solved separately with its distinct carbon cap constraint. The next sections describes the algorithm.

5.2 Algorithm to Solve Decomposed VI

Instead of a coupling constraint for all the DUE-episodes in an analysis we can distribute the carbon caps among the DUE-episodes. This implies that each DUE-episode can be solved separately with its own carbon cap constraints. Further, we assign the carbon caps specific to each user class and each OD pair. A useful property of our problem is that its feasible region Ω can be expressed as a Cartesian product of a set of closed and convex linear constraints: demand satisfactory and carbon cap conditions. This naturally leads to a decomposition optimization scheme to solve this problem. The algorithm proposed by Zhan and Ukkusuri (2014) decomposes the original VI problem coupled variation inequalities of lower dimensions, with each defined for a user group and origin-destination pair. The algorithm ensures the mapping finds a convergent sequence and it can be proved that such a fixed point is a solution for sub-VI problem. If we find a set of solutions for all sub-VI problems simultaneously, it can be shown that the combined solution is a solution of the original VI problem.

Algorithm steps (Zhan and Ukkusuri 2014):

Step 0: Set counter $k=0$. Initialize a feasible departure rate.

Step 1: Run the simulation $CTM(\gamma^k)$ and compute $TC(\gamma^k)$, $CC(\gamma^k)$, $GC(\gamma^k)$.

Step 2: Decompose $\gamma^k = (\gamma_1^k, \gamma_2^k, \dots, \gamma_m^k)^T$.

Step 3: Find the $\lambda^k(\gamma^k)$ that ensures most number of user classes and OD pairs satisfy: $\|T_i(\gamma_i^k) - T_i(\gamma_i^{k-1})\| \leq \alpha \|\gamma_i^k - \gamma_i^{k-1}\|$, in which $T_i(\gamma_i^k) = Pr_{\Omega_i}[\gamma_i^k - \lambda^k(\gamma^k)GC_i(\gamma^k)]$

Step 4: Update departure rate γ_i^k using mapping T_i only for those user classes and OD pairs that satisfy the condition in Step 3. For others that not satisfied, set $\gamma_j^k = \gamma_j^{k-1}$.

Step 5: If none of the user classes and OD pairs are found satisfy condition in Step 3, set $\gamma_j^k = \gamma_j^{k-1}$, $\lambda^k(\gamma^k) = \lambda^{k-1}(\gamma^{k-1})/2$.

Step 6: If $\|z^* - \gamma^k\| \leq \epsilon$, terminate the algorithm, $\gamma^* = z^*$. Otherwise $\gamma^{k+1} = \gamma^k$, Set $k = k + 1$, go to step 1.

6 Numerical Example

We solved the PMCA-DUE model with two test networks.

- X-shape network (similar to that used in Ukkusuri et al. (2012)) with four O-D pairs and three user classes. The network has ten cells and the equilibrium is based on departure time choice only.

- (b) Sioux-Falls network with six O-D pairs and five user classes. The network has 114 cells and 142 links. There are two O-D pairs with three paths, two O-D pairs with two paths, and two O-D pairs with a single path.

Each link in the network is divided into multiple cells. The time step for the simulation is set such that no vehicle can move more than one cell in a single time step. We choose the time step as 60 seconds. With free flow speed 30 miles/hour, the maximum length of a cell is 0.5 miles or 0.8 kilometers. Assuming saturation flow as 1800 vehicles per hour per lane the maximum flow rate for a cell is 30 vehicles per time step per lane. At saturated condition the bumper-to-bumper distance is about 10 meter. Therefore, the jam density is $(0.8 \cdot 1000)/10$ or 80 for the cells in the network. Other than source and sink cells we use these parameters for all cells in the network. The ratio to forward to backward shockwave propagation is 0.8 in the analysis. The convergence criterion is the norm of difference between two consecutive solutions. All results in this research are obtained by setting the convergence criterion as 0.05. The optimal value of parameter step size in projection algorithm that produces the best results is different for different problems. We observe that the value is less than 1 in all cases and ranges between 0.1 and 0.625 in our tests.

6.1 Input Parameters

To quantify the carbon cost we extracted a relationship between average path speed and GHG emissions rate (g of CO₂ per mile) using the county level database from EPA-MOVES. We tested our algorithm on Sioux-Falls network which is closer in terms of traffic and atmospheric conditions of Minnehaha county of South Dakota in the U.S. EPA-MOVES provides access to county level data that include fuel type and formulation, vehicle age distribution, temperature profile, humidity, and fuel type distribution. With link geometry attributes identical to the Sioux-Falls network, we estimate GHG emissions for different speed levels. A fourth-order polynomial fits the data points and represents the relationship between average path (trip) speed and GHG emissions. The fitted relationship is similar to the empirical relationship obtained in the study by Barth and Boriboonsomsin (2008). Gardner et al. (2013) followed similar approaches to extract functional relationship from EPA-MOVES. The fitted function is as follows:

$$\psi_e = 0.0002v^4 - 0.0417v^3 + 2.8745v^2 - 87.317v + 1323.5. \quad (19)$$

Here, ψ_e = Emissions rate g/mile and v = Average speed in miles/hour. We used this equation for both X-shape and the Sioux-Falls network (Fig. 3).

6.1.1 Trip Demand and Value of Time

We consider three income classes with three types of trips for our tests. Number of trips for user groups representing different income levels are obtained from the 2009 National Household Travel Survey data and are listed in Table 1. To account for the heterogeneity in travel cost for each income class we use the value of travel time

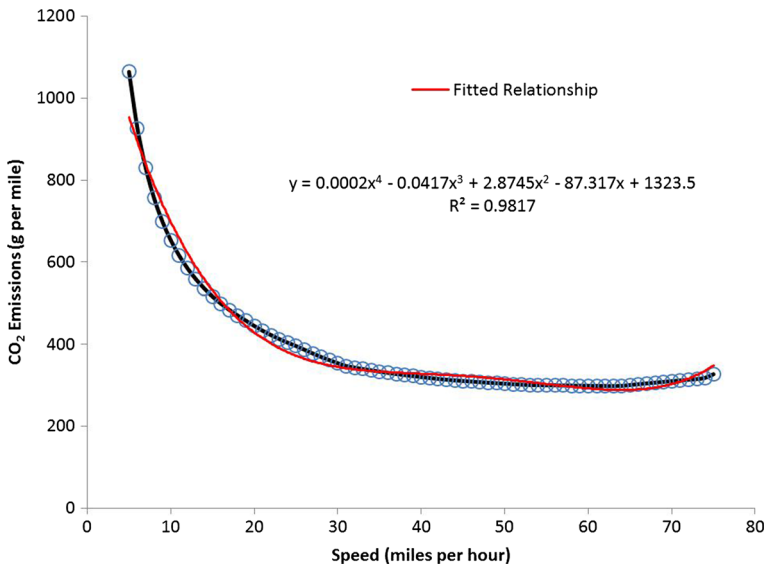


Fig. 3 Fitted relationship between speed and emissions rate for Minnehaha County, SD using EPA-MOVES data

(VOTT) for trips specific to purpose. The VOTT values are obtained from the guidelines provided by FHWA (US DOT R 2011). For the ease of conducting experiments, the number of total trips are proportioned with the same relative difference among the groups.

6.1.2 Parameters for Cost Function

Table 2 shows the parameters used for cost function. The parameters correspond to: travel cost, carbon cost, effect of remaining carbon credits relative to initial allocation at the point of decision making, and available money to spend in the carbon market

Table 1 User group definition

User Group	Income Range	Work Trips	VOTT Work	Grocery Trips	VOTT Shopping	Rec. Trips	VOTT Rec.
Group-1	\$20,000 - \$39,999	4	7.2	7	5.8	3	6.1
Group-2	\$40,000 - \$59,999	6	12.0	8	9.6	4	10.2
Group-3	\$60,000 - \$99,999	7	18.0	10	14.4	5	15.3

Table 2 Parameters for generalized cost function (Aziz et al. 2015)

User	β_{TC}	β_{CC}	β_{RB}	β_{HH}
Class-1	0.031	0.056	-0.42	-0.048
Class-2	0.0066	0.113	3.72	1.163
Class-3	0.011	0.057	2.75	-1.63
Class-4	0.024	0.46	5.23	1.04
Class-5	0.03	0.109	1.52	-1.72

relative to initial money. The details of the estimation procedure can be found in Aziz et al. (2015).

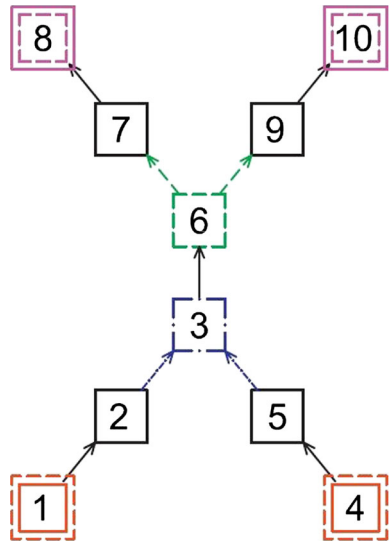
6.2 X-Network

The X-shape network, originally used in Ukkusuri et al. (2012), is a small network with diverge and merge cells (Fig. 4). It allows to test the equilibrium with departure time choice. We define a scenario with three DUE episodes characterized by distinct trip demand for each user class. The carbon cap constraint requires a threshold value for the PMCA-DUE problem as a whole (i.e., coupled with all DUE-episodes). First, we solve three DUE problems without carbon cap constraints separately and compute the carbon consumption. Then we set a 2 % reduction goal for the PMCA-DUE and define the constraint such that the total carbon consumption for all three DUE-episodes cannot exceed 98 % of the base case. We solve the network following both approaches described earlier in Sections 5.1 and 5.2. Results from two solution approaches are compared to verify whether significant difference exists between the solution approaches.

The Figs. 5, 6 and 7 show the results obtained from basic projection Algorithm 5.1. The departure rate vs. generalized cost plots show that the highest departure rate occurs at the lowest cost. This trend is valid for all user classes and O-D pairs. Next, the Figs. 8, 9 and 10 show the results obtained from decomposed VI projection Algorithm 5.2. No significant differences are found in the cost vs. departure rate plots compared with those obtained from the basic projection algorithm with coupled constraints.

Table 3 summarizes the results. The base case represents the problem without any carbon cap, basic refers to the solution obtained by basic projection algorithm and coupled carbon cap constraint, and decomposed refers to the solution obtained by the decomposed VI algorithm with individual carbon cap constraints. At system level we see the total carbon consumption reduced to near 2 % for all DUE-episodes. In other words, the constraint is not active. It is interesting to see that the travel cost is lower with carbon cap constraint for DUE-1 when compared with the base case. Due to the inclusion of carbon credit cost into the generalized cost, the path flows are redistributed and this may cause a lower total cost compared with the base case. These findings are same for both basic and decomposed algorithms. However for

Fig. 4 Cell representation of X-Shaped Network (Ukkusuri et al. 2012)



DUE-2 and DUE-3, the travel time costs increase when the carbon cap constraints are introduced. As mentioned earlier, path flow redistribution is one of the possible causes that affects the resulting travel times. In addition, demand levels specific to user classes also affect the travel costs.

Table 4 reports the cumulative carbon cost difference at O-D level for each user class using the results obtained from basic and decomposed algorithms. In the tables, each row represents a user class and each column represents an O-D pair. Each cell value indicates the difference between the solution obtained from basic projection and decomposed algorithm. The purpose of the comparison is to show that the results obtained from decomposed algorithm that solves a relaxed version of the problem (i.e., no coupled constraint rather carbon caps at individual level) are not significantly

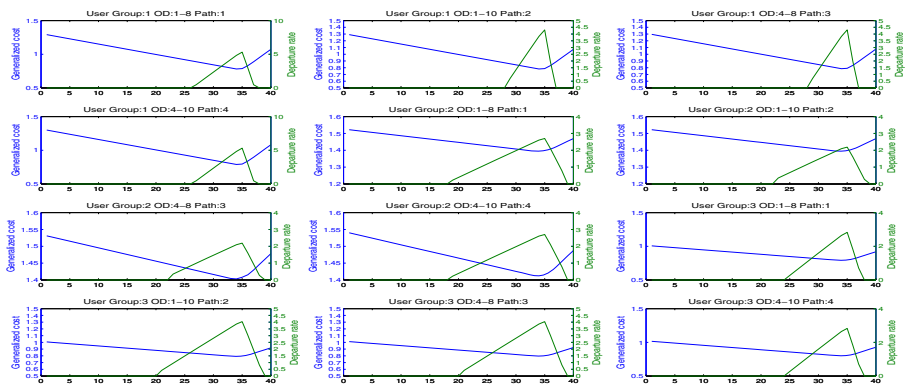


Fig. 5 Results for DUE-1: Coupled constraint problem

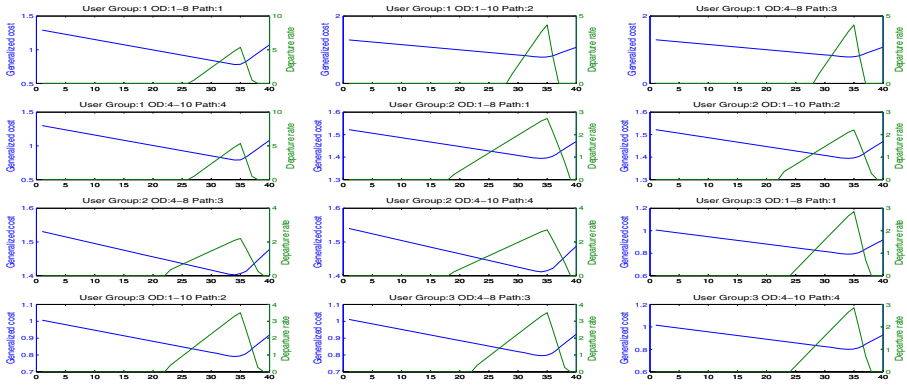


Fig. 6 Results for DUE-2: Coupled constraint problem

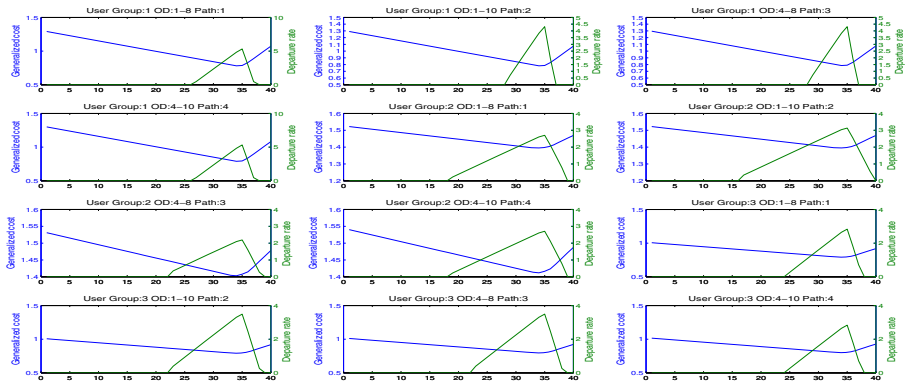


Fig. 7 Results for DUE-3: Coupled constraint problem

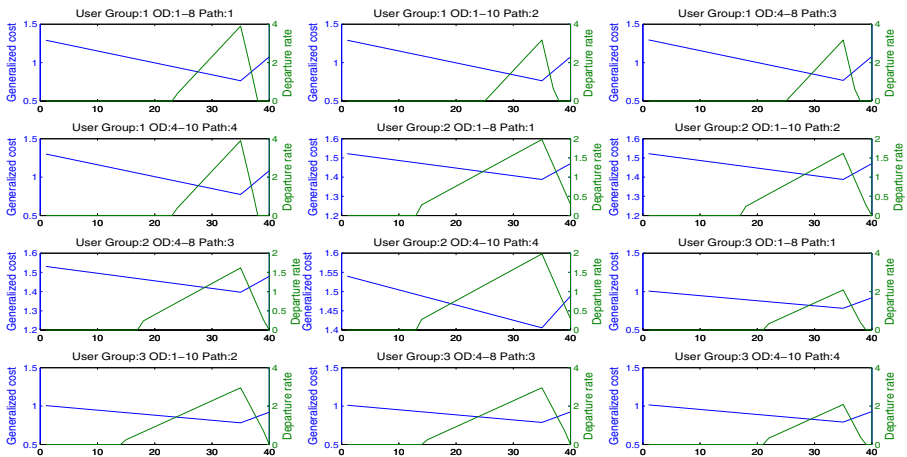


Fig. 8 Results for DUE-1: carbon constraint at OD level

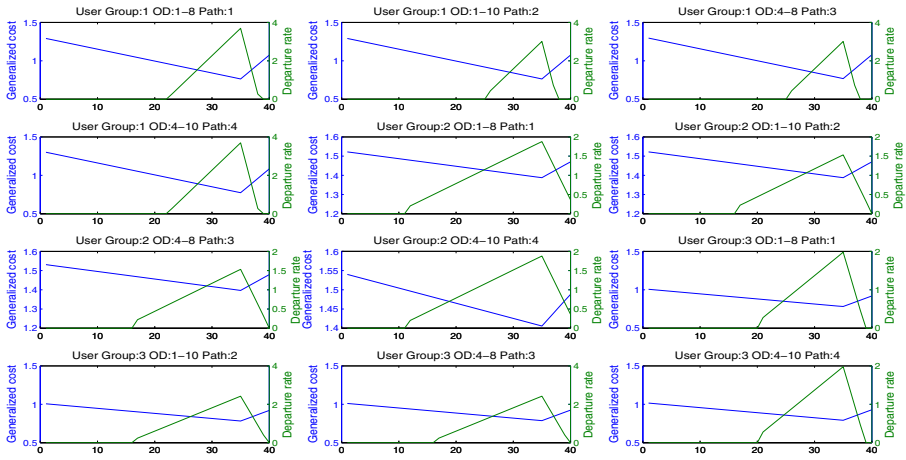


Fig. 9 Results for DUE-2: carbon constraint at OD level

different from the solutions from basic projection algorithm. From the tables we observe that:

- (a) The decomposed algorithm underestimates the carbon consumption at OD level. This is valid for all three episodes and all user classes. However the extent of underestimation is negligible.
- (b) The highest difference we obtain is 0.114 %. Most cases the difference is below 0.05 % that is negligible.
- (c) For user class-1 the differences are high (≤ 0.114 %) for DUE-episodes.

With evidences from the cost vs. departure rate plots, the total time and cost values, and the carbon cost difference values at group levels, we conclude

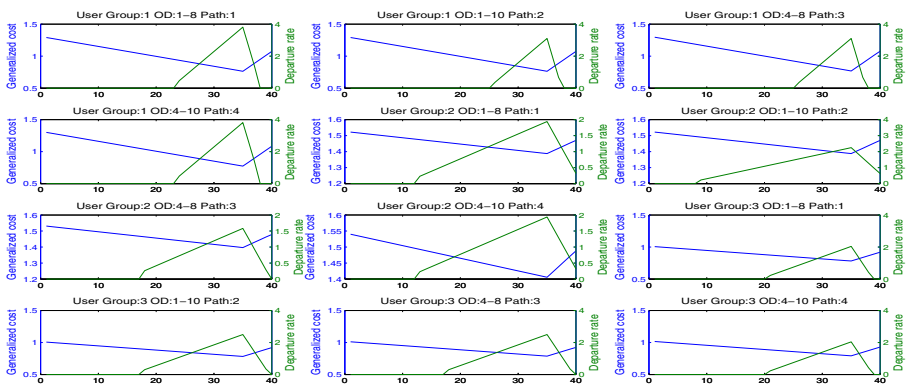


Fig. 10 Results for DUE-3: carbon constraint at OD level

Table 3 System level results for X-network with coupled and decomposed approaches (2 % carbon reduction constraint from base)

Episode	Carbon cost			Travel cost		
	Base	Basic	Decomposed	Base	Basic	Decomposed
DUE-1	393600	386000	385810	2972	2711	2788
DUE-2	370200	361900	361747	2431	2686	2740
DUE-3	394500	385900	385723	2887	2944	2955

that the results obtained from decomposed algorithm are not significantly different from the basic projection algorithm. This is important because the basic projection algorithm does not solve the reasonably sized networks efficiently whereas the decomposed algorithm can solve those networks at desired error tolerance.

Figure 11 shows the convergence for the DUE-1, DUE-2, and DUE-3 for the X-network and we can see stable convergence is achieved for each case. The next section describes the results from Sioux-Falls network obtained through the decomposed VI algorithm.

Table 4 Comparison between two solution approaches: basic vs. decomposed algorithm

User	Carbon cost		Difference(%)		From basic projection algorithm	
	OD-1	OD-2	OD-3	OD-4	OD-3	OD-4
DUE-1						
Class-1	-0.114	-0.115	-0.105	-0.098	-0.105	-0.098
Class-2	-0.038	-0.009	-0.005	-0.031	-0.005	-0.031
Class-3	-0.041	-0.0632	-0.058	-0.028	-0.058	-0.028
DUE-2						
Class-1	-0.084	-0.086	-0.078	-0.072	-0.078	-0.072
Class-2	-0.025	-0.004	-0.0005	-0.019	-0.0005	-0.019
Class-3	-0.019	-0.037	-0.034	-0.01	-0.034	-0.01
DUE-3						
Class-1	-0.108	-0.112	-0.103	-0.093	-0.103	-0.093
Class-2	-0.034	-0.043	-0.005	-0.026	-0.005	-0.026
Class-3	-0.034	-0.055	-0.049	-0.022	-0.049	-0.022

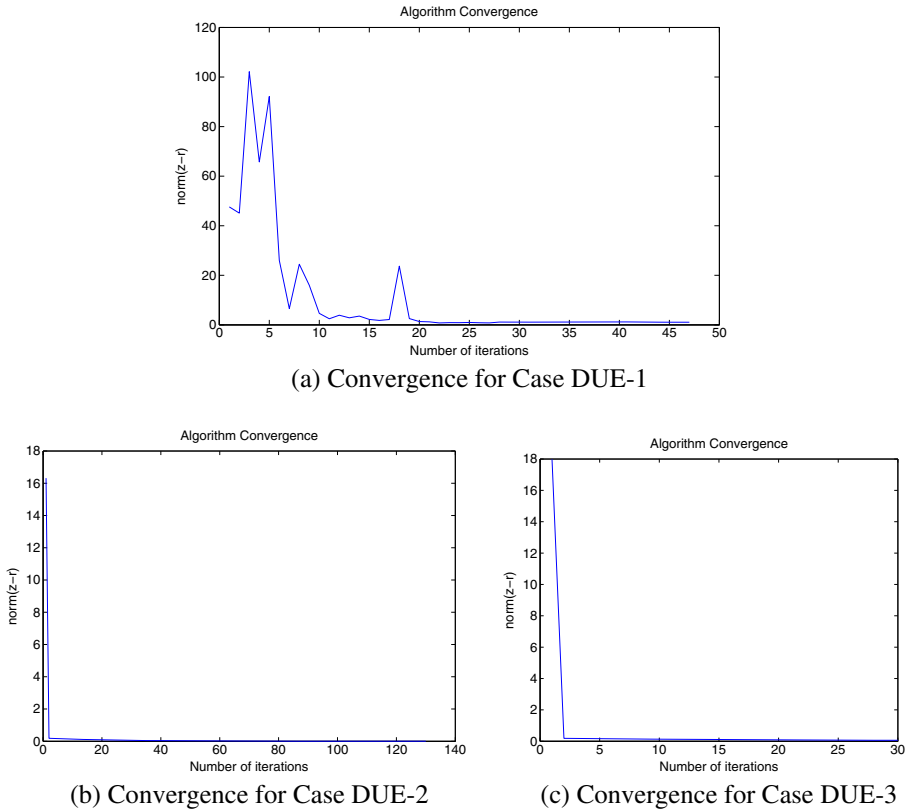


Fig. 11 Convergence for X-network

7 Results for Sioux-Falls Network

This section reports the results for Sioux-Falls network. The six O-D pairs are: 540-550, 551-541, 540-570, 551-570, 571-541, and 571-550. For each O-D pair and each user class we define the trip demands to characterize the DUE-episodes. A three-episode PMCA-DUE is analyzed using the decomposed VI algorithm. Five user classes are defined: (a) Low income and work trip, (b) Medium income and work trip, (c) Medium income and grocery trip, (d) High income and work trip, and (e) High income and grocery trip. The value of travel time is used as a measure of the income level. The relative value of carbon cost is capture through the generalized cost function parameters. These parameters are estimated using the data obtained from experimental games (Aziz 2014).

The decomposed VI algorithm solves each DUE-episode separately. For brevity, we report the results for DUE-1 (Fig. 17) episode here and the results for DUE-2 (Fig. 18) and DUE-3 (Fig. 19) can be found in the Appendix C. We test the PMCA-DUE model for 2 %, 5 %, and 7 % carbon reduction from the base case where no carbon cap is introduced. First we report the cost vs. departure time plots for DUE-1

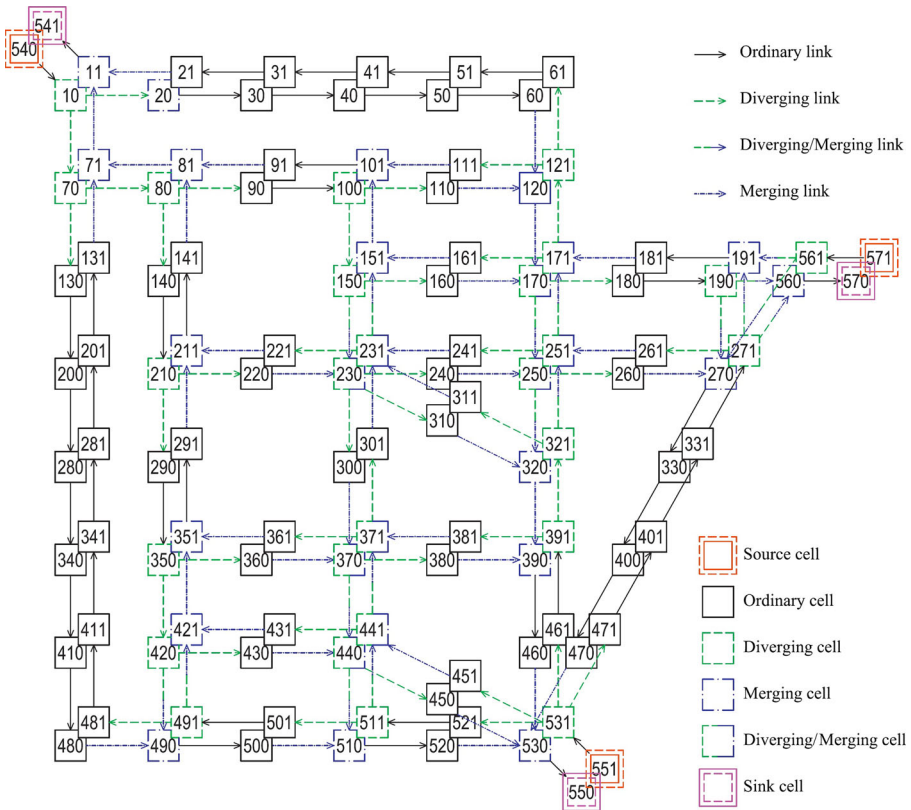


Fig. 12 Cell representation of SiouxFalls network (Ukkusuri et al. 2012)

at 2 %, 5 %, and 7 % reduction to examine the equilibrium conditions. Then we compare the O-D level carbon and travel time costs for each user class for each reduction level. The base case for DUE-1 can be found in the Appendix C (Fig. 12).

7.1 Measuring Convergence

A well-recognized convergence metric is Relative Gap. Relative Gap compares current assignment solution to the ideal shortest-path cost for all O-D pairs and departure intervals. We followed the recommendations in FHWA guide on dynamics traffic assignment (Sloboden et al. 2012) and the DTA Primer (DTA 2011). The relative gap can be computed as follows:

$$\text{Relative Gap} = \frac{\sum_{t \in T_f} \sum_{m \in M} \sum_{w \in W} \sum_{p \in P^w} (GC_{p,t}^m * r_{p,t}^m) - \sum_{t \in T_f} \sum_{m \in M} \sum_{w \in W} (d_{w,t}^m * U_{w,t}^m)}{\sum_{t \in T_f} \sum_{m \in M} \sum_{w \in W} (d_{w,t}^m * U_{w,t}^m)}$$

$d_{w,t}^m$ = Demand for OD pair w for class m at departure time t

$U_{w,t}^m$ = Shortest generalized cost for OD pair w for class m at departure time t

Table 5 Relative gap values at OD and system level for DUE-1

Level	DUE-1-98	DUE-1-95	DUE-1-93
<i>OD-1</i>	0.002	0.008	0.002
<i>OD-2</i>	0.0000004	0.0000002	0.0000003
<i>OD-3</i>	0.009	0.005	0.0012
<i>OD-5</i>	0.007	0.003	0.0014
<i>System</i>	0.0042	0.0048	0.001

Tables 5 and 6 show the relative gaps for DUE-1, DUE-2, and DUE-3 episodes. The values are reasonably small.

7.2 PMCA-DUE-1 with 2 %, 5 %, and 7 % carbon reduction

The total carbon cap is set at 98 %, 95 %, 93 % level of the base case for each case respectively. Further, the cap is distributed at O-D level for each group. We cannot distribute the carbon cap uniformly because each user class has a unique generalized cost as a parametric combination of carbon cost and travel cost. Therefore, we compute the carbon consumption of each user class for each O-D pair in the base case and set the carbon caps accordingly. Figure 13 reports the generalized cost vs. departure rate plots for the PMCA-DUE-1 with 2 % reduction level. The plots show consistency in terms of the feature that higher departure rate occurs at lower cost reflecting DUE conditions. For few cases we observe multiple peaks in the departure rate vector. Most of those cases are accompanied with multiple troughs in the cost vector. Whenever the cost falls, the departure rate goes up. For user class-4 and class-5, this is more prominent. Similar trends can be found for the DUE-episodes with 5 % and 7 % reductions. For PMCA-DUE-1 at 7 % reduction, we see multiple peaks in the departure rate vector more often. Since the carbon constraint becomes tight it may happen that the rate vector is distributed over multiple peaks to satisfy equilibrium.

Table 6 Relative gap values at OD and system level for DUE-2 and DUE-3

Level	DUE-2-98	DUE-2-95	DUE-3-98	DUE-3-95
<i>OD-1</i>	0.002658	0.00323	0.000338	0.004916
<i>OD-2</i>	0.002151	0.005906	0.00002515	0.00588934
<i>OD-3</i>	0.0007335	0.002988	0.0053304	0.004992
<i>OD-5</i>	0.0033899	0.021703	0.00002363	0.01502255
<i>System</i>	0.0023	0.009	0.000955	0.006347

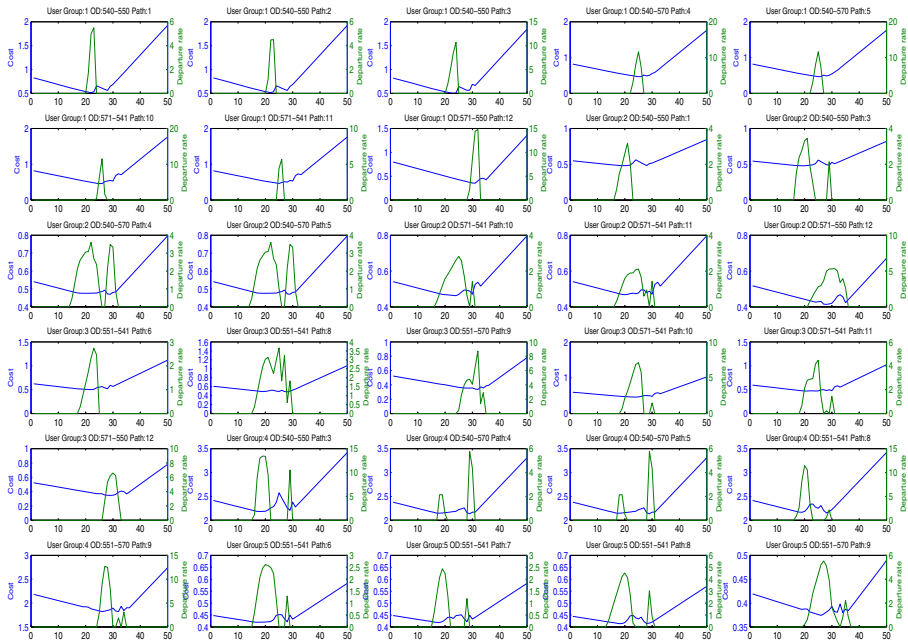


Fig. 13 PMCA-DUE-1 results: 2 % reduction from base case

7.3 Comparison of OD Level Carbon and Travel Cost at Different Levels of Carbon Reduction

This section compares the total carbon and travel cost at O-D level when PMCA is implemented at different reduction level. The goal here is to explore the effect of PMCA on total carbon consumption and system-wide travel costs. Note that travel cost is not same as generalized cost. Travel cost is defined as the total cost accounting for travel time and penalties for early and late arrivals. The travel cost comparison shows the impact of PMCA when personal carbon allowance is introduced in the system. We only compare the results for OD-1, OD-2, OD-3, and OD-5. Since OD-4 and OD-6 do not have any path choices, the results are not reported here. Table 7 summarizes the results at O-D level. Carbon consumption at O-D level goes down as carbon cap constraints are introduced. This is valid for all O-D pairs and all reduction levels. The increase in travel cost is much higher as the carbon cap goes from 5 % to 7 %. This trend holds true for all O-D pairs. This indicates a non-linear pattern of travel cost increase as PMCA imposes carbon constraint.

For OD-2, the travel cost first decreases with 2 % reduction. However, the travel cost increases as the reduction level rises. This can be explained by the effect of path flow redistribution and the conflicting nature of travel and carbon cost. With a smaller carbon cap, the PMCA-DUE model redistributes the flow to equilibrate the generalized cost that include both carbon and travel time cost. It is possible that this

Table 7 OD level cost comparison at different levels of carbon caps

		Carbon Reduction			Cost level			
		2 %	5 %	7 %	Base	2 %	5 %	7 %
Case:	Base	2 %	5 %	7 %	Base	2 %	5 %	7 %
OD-1	56000	53261	53378	52600	3407	3424	3496	3739
OD-2	58651	53272	53268	52575	2671	2646	2687	2848
OD-3	51692	49737	49113	48980	4116	4119	4230	4978
OD-5	45756	43636	42807	42730	2534	2514	2576	2658

results into a better flow distribution in terms of O-D level cost. However, with a higher cap, the model redistributes the flow so that carbon cap constraint is satisfied resulting into a higher travel cost compared with the base case. OD-5 exhibits the same feature (Figs. 14 and 15).

7.4 Comparison of Carbon Consumption for User Classes

Five user classes are defined with three attribute: (a) income level (value of travel time), (b) how many trips to make each week?, (c) purpose of the trip. The classes are: 1. Low income, fewer weekly trips and work trip, 2. Medium income, moderate

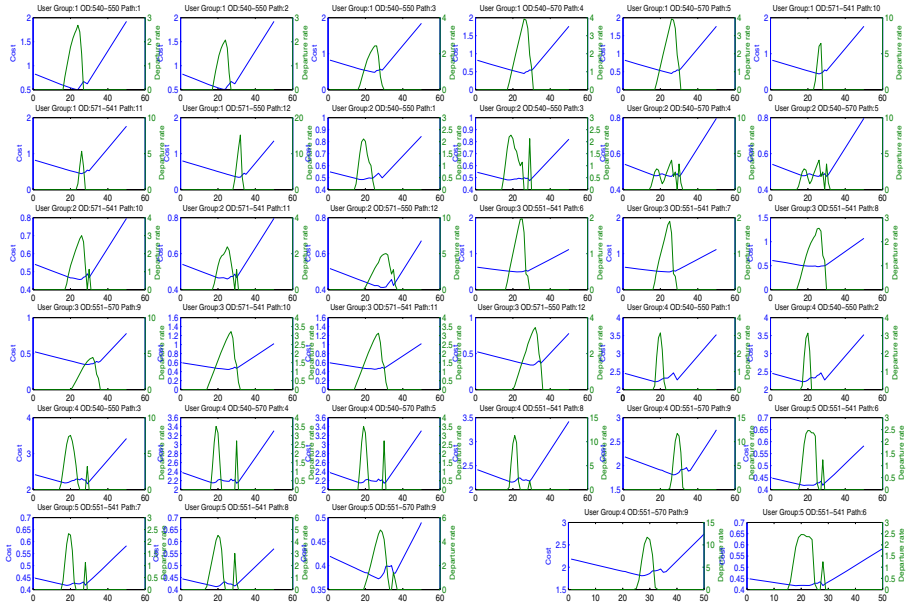


Fig. 14 PMCA-DUE-1 results: 5 % reduction from base case

weekly trips, and work trip, 3. Medium income, moderate weekly trips, and grocery trip, 4. High income, high weekly trips, and work trip, 5. High income, high weekly trips, and grocery trip. The DUE-1 episode is the morning peak hour with work trips and grocery trips specific to OD pairs. Table 8 shows the total carbon consumptions for each user class. The results are categorized by OD pair and level of carbon reduction to demonstrate the effects of PMCA. The table reports % change only when the consumption is significantly large.

The decrease in carbon consumption for class-4 is much smaller compared with class-5 as seen in the results for OD-1 and OD-3. Class-4 and class-5 are differentiated by only trip purpose. For work trips the reduction level is smaller. The largest decrease is 1.82 % as observed for OD-3. On the other hand, the decrease for grocery trips ranges between 6-7.4 %. This is intuitive because class-5 users have a high value of travel time for work trips compared with grocery trips. It is more likely that the users would be saving carbon credits more in the grocery trips.

The carbon consumption for class-2 gets smaller significantly (ranging from 7-11 %) as carbon caps are introduced. However, the relative changes from 2 % to 5 % and 7 % reductions are smaller. It is interesting to see that the reduction in carbon for grocery trips by class-3 (medium income) users is smaller compared with class-5 (high income). Higher income (class-4 and class-5) users are characterized with higher trips compared to medium income (class-2 and class-3). It is more likely that higher income users (class-5) would be more sensitive to carbon saving in grocery trips compared with medium income users (class-2).

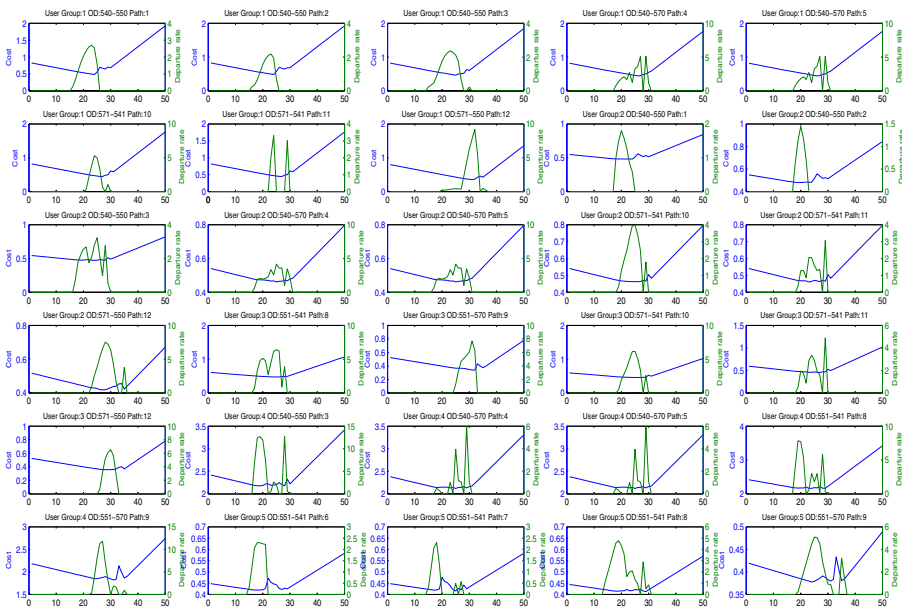


Fig. 15 PMCA-DUE-1 results: 7 % reduction from base case

For class-1 users the carbon consumption decreases with higher carbon caps with the exception in OD-1. This can be explained by flow distribution mechanism at equilibrium. The value of time is low for class-1 users compared with other users. Equilibrium condition at the base case will push more flows from user class-1 to a relative higher travel time option (rate vector) resulting into lower carbon. With the carbon caps, the equilibrium state considers both carbon and travel costs. Accordingly, it is possible that flows from other user class are pushed to low-carbon (higher travel cost) option. This may cause higher carbon cost for the travel option compared to the base and the carbon consumption goes up for all classes using the travel option (specifically the users from class-1).

7.5 Comparison of Path Level Carbon Cost (Emissions)

This section explores the changes in carbon cost specific to paths. The cumulative carbon cost is a parametric measure of the emissions level of the particular path contributed by a particular user class. We define 100 g of CO₂ equivalent to one carbon credit and the cost can be directly converted into emissions. One particular interest is to observe the change in the level of emissions at path levels. It is possible that the

Table 8 Comparison of carbon consumptions for different user classes (values in the parentheses show the difference in % from base)

OD-Pair	Total		Carbon	Cost	
	Class-1	Class-2	Class-3	Class-4	Class-5
OD-1(Base)	18082	14620	363	22567	363
OD-1-98	16379 (9.4 %)	13038 (10.8 %)	368	22454 (0.5 %)	362
OD-1-95	16802 (7.07 %)	13053 (10.72 %)	361	22400 (0.73 %)	361
OD-1-93	17160 (5.1 %)	12964 (11.3 %)	373	22409 (0.69 %)	357
OD-2(Base)	23444	24906	348	9605	348
OD-2-98	20357 (13 %)	22622 (9.17 %)	350	9600	343
OD-2-95	19987 (15 %)	22905 (8.03 %)	359	9675	343
OD-2-93	19487 (17 %)	22674 (8.96 %)	352	9718	344
OD-3(Base)	414	415	17033	13127	20704
OD-3-98	387	365	16604 (2.51 %)	13009 (0.89 %)	19371 (6.4 %)
OD-3-95	375	368	16303 (4.28 %)	12889 (1.82 %)	19178 (7.3 %)
OD-3-93	369	368	16213 (4.81 %)	12865 (2 %)	19167 (7.4 %)
OD-5(Base)	11069	14109	19871	353	353
OD-5-98	10232 (7.55 %)	13071(7.35 %)	19637 (1.18 %)	352	344
OD-5-95	9868 (10.85 %)	12903 (8.55 %)	19340 (2.67 %)	352	344
OD-5-93	9736 (12.04 %)	12965(8.11 %)	19438 (2.18 %)	349	343

emissions level of a path significantly increases or decreases due to distribution of flows as PMCA-DUE satisfies equilibrium. Figure 16 shows the changes in carbon consumption(i.e., cumulative carbon cost) at path level for all O-D pairs.

For OD-1 (Fig. 16 top-right) the carbon consumption for path-3 decreases as we set the carbon consumptions caps. At the same time, the carbon consumptions go up for path-1 and path-2. This trend continues up to 5 % of reduction and at 7 % reduction path-3 exhibits similar carbon consumption as that of 5 %. However, the consumption is higher for path-1 and lower for path-2 when compared with 5 % reduction level results.

For OD-2 (Fig. 16 bottom-right), flows are distributed between two paths. Lower carbon consumption can be observed when carbon cap constraints are introduced. The carbon consumptions do not vary much at different levels of carbon cap. For OD-3 (Fig. 16, bottom-left) The total carbon consumptions increase for path-1 and path-2, whereas path-3 shows lower carbon consumption. The pattern changes for the case with 7 % reduction. The carbon consumption goes up for path-3 while going down for path-2 and path-3. OD-5 (also with two paths) shows a different pattern compared with OD-2 (Fig. 16, top-left). The carbon consumption is higher for path-2 at 2 % and 5 % reduction level and is lower for 7 % reduction level.

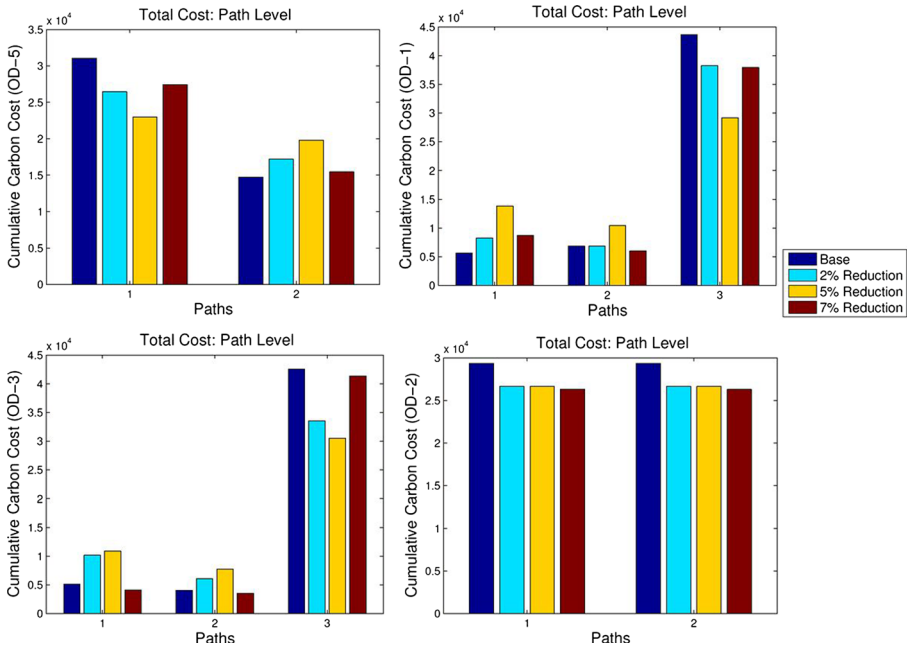


Fig. 16 Path level carbon cost at different carbon caps

8 Concluding Remarks

The PMCA-DUE model is one of the first dynamic user equilibrium models incorporating the travel behavior under carbon allowance scheme. The complementarity based formulation provides a novel way to describe equilibrium under PMCA scheme. Consideration of carbon cost in addition to travel cost for path and departure time choice requires a new generalized cost function and equilibrium condition. Addressing this, we have developed a multi-user dynamic equilibrium model where each user class has a distinct value of travel time, trip demand, different sensitivity to perceived carbon cost (see Section 4.4). Also, the effects of initial allocation of carbon credits, value of travel time, and number of trips are considered in the generalized cost function. This research makes several contributions to the literature. First, a multi-class network equilibrium model is formulated. Both complementarity and equivalent VI formulation are demonstrated. Second, we propose two solutions techniques: basic projection and decomposed VI algorithms. We solve two test networks and analyze the results. Third, the user and OD level travel and carbon costs are investigated. Carbon consumption patterns are explored. Finally, the impact PMCA scheme is investigated which provides insights for carbon allowance schemes in general. The key findings from the analyses are as follows:

- (a) Introducing carbon cap through PMCA schemes can lower the system level travel time up to certain level of cap. Our results (Tables 3 and 8) show that the cumulative travel costs are lower from the base case when PMCA scheme is in effect. This can be explained from the concept of congestion pricing and the conflicting nature of travel time minimization and carbon credit consumption. When the average trip speed is high, the carbon cost goes up. At the same time, the travel cost goes down. Since the generalized cost in our model considers both, the model distributes the flows such a way that the generalized cost, which is a parametric combination of the carbon and travel cost, is minimized. At equilibrium it redistributes the flow by adjusting the departure rate vector. This results into a new equilibrium state with lower cumulative travel cost for a class. This does not necessarily decrease the travel cost for each path. Rather for some paths the costs increase and for some paths the cost decrease as exhibited by the Fig. 16. As a net effect, it is possible to have lower travel cost for the system at OD level.
- (b) Class-4 users (characterized by high value of travel time) are less sensitive to carbon constraint in the context of work trips. Relatively higher value of time and higher penalties for late and early arrival may cause to exhibit this. For work trips class-4 users do not show significant reduction of carbon consumption as the carbon cap goes from 2 % to 7 %.
- (c) One important finding from our results is that the emissions level (parametric function of the carbon consumption) for paths changes with the levels of reduction. For air quality conformity this is important because PMCA leads reduction in carbon consumption for the network, however for some paths the emissions can be higher as seen in Fig. 16.

- (d) Carbon consumptions are lower for cases (OD-3) characterized by grocery trips compared with cases (OD-1) characterized by work trips. This is mainly because of the nature the parameters in the generalized cost function. The parameters specific to grocery trips prioritize the savings of carbon credits so that it can be used for work trips later.
- (e) Our analysis indicates that the equilibrium state highly depends on the composition of trips characterized by purpose. A case with higher grocery trips will reach a different equilibrium compared with a case with higher work trips. This is because of the heterogeneity captured through the generalized cost function parameters.
- (f) The results also show the impact of setting initial distribution of carbon credits. The initial distribution is incorporated through the carbon cap constraint in the model. As we move from 5 % to 7 % reduction, the equilibrium state changes and we observe a new path cost pattern (see Fig. 16) and the OD level carbon consumptions are also affected (see Tables 3 and 8).

8.1 Implementation Challenges

The real world implementation of the PMCA scheme asks for building the infrastructure for PMCA system. This includes automating the transactions and regulating the distribution of the credits so that the system sustains. Further, one needs to assess the economic feasibility of the PMCA installation at different jurisdictional levels. Another major challenge will be the public acceptance at the initiation of the scheme. The authority needs to promote the scheme with clarity such that the system users of all classes can readily see the benefits. With emergent paradigm of connected automated vehicles, we expect that the PMCA execution can leverage the communication among the vehicles and infrastructures in terms of transaction, system regulation, and maintaining carbon market stability.

8.2 Limitations and Future Directions

This research has few limitations in terms of scope and transferability. First, the parameters for the generalized cost function are estimated specifically for the Sioux-Falls network. Although the models are applicable to other networks, one must estimate parameters specific to the transportation network. Second, the captured heterogeneity across population can be extended to more generally by considering other trip types, finer level of income, and vehicle composition.

Finally, our solution technique solves only up to 7 % reduction for the Sioux-Falls network. It is possible that the problem becomes infeasible with higher carbon cap. We observe that the problem can be solved with lower trip demand keeping the carbon cap same indicating the allocated carbon for the system may not be sufficient for the original demand. The demand feasibility issue can be resolved through redistribution of the carbon credits based on the demands for specific groups at specific OD pairs. This alludes to another research question regarding the initial allocation of carbon credits with efficiency and equity. This is a potential future research direction that is critical for the implementation of the PMCA schemes.

Acknowledgments This material is partly based upon work supported by the National Science Foundation under Grant No. 1017933. Any opinions, findings, and conclusions or recommendations expressed in this material are those of the authors and do not necessarily reflect the views of the National Science Foundation.

Appendix A: Appendix Cell transmission model

The CTM divides each link of the network into finite number of homogeneous cells. Each cell has a length at least equal to the distance traveled in a single time interval at free flow speed. Also, the time horizon is finite and discretized into a number of intervals.

(a) Notations and symbols:

Indices:

- w : index of origin-destination pairs, $w \in \mathbb{W} : \{1, \dots, W\}$;
- p : index of paths, $p \in \mathbb{P} : \{1, \dots, P\}$;
- i, j, k : index of cells;
- t : index of discrete time intervals,
- m : index of user group, $m \in \mathbb{M} : \{1, \dots, M\}$.

Parameters:

- α_1^m : unit cost of travel time for user class m ;
- α_2^m : unit cost of early arrival for user class m ;
- α_3^m : unit cost of late arrival for user class m ;
where $\alpha_2^m < \alpha_1^m < \alpha_3^m$;
- t^{*w} : preferred arrival time for O-D pair w (this is same for all user classes);
- β_T^m : Estimated parameter for travel time cost in the generalized cost function for class m ;
- β_C^m : Estimated parameter for carbon cost in the generalized cost function for class m ;
- β_R^m : Estimated parameter for the effect of remaining carbon budget for class m ;
- β_H^m : Estimated parameter for the effect of available money to spend in the carbon market for class m ;
- $d^{w,m}$: total demand from O-D pair w for class m ;
- ζ : infinitesimal flow to avoid zero denominator;
- t_e : maximum departure time (loading time);
- t_f : maximum time horizon (network clearance time);
- N^i : jam density of cell i ;
- Q^i : flow capacity out of cell i ;
- δ : ratio of backward to forward shockwave propagation.

Sets:

- C : set of cells;
- C_O : set of ordinary cells;
- C_R : set of source cells;
- C_S : set of sink cells;
- C_D : set of diverging cells;
- C_M : set of merging cells;

- E : set of links or cell-connectors;
- E_O : set of ordinary links;
- E_D : set of diverging links;
- E_M : set of merging links;
- Γ_i^{-1} : set of predecessors of cell i ;
- Γ_i : set of successors of cell i ;
- M : set of all user classes;
- W : set of all O-D pairs;
- P^w : set of paths for O-D pair w ;
- P : set of all the paths, $P = \cup_{w \in W} P^w$,
- T_e : set of all departure time intervals, $T \triangleq \{0, \dots, t_e\}$
- T_f : set of all time intervals, $T_f \triangleq \{0, \dots, t_f\}$.

Variables:

- $x_{p,t}^{i,m}$: cell occupancy of cell i at time t for the flow on path $p \ni i$ for user class m ,
- $y_{p,t}^{i,j,m}$: flow from cell i to cell j at time t for the flow on path $p \ni (i, j)$ for user class m ,

- \bar{x}_t^i : aggregate cell occupancy of cell i at time t , i.e., $\bar{x}_t^i = \sum_{\forall p \ni i} x_{p,t}^{i,m}, \forall i \in C; t \in T_f$,
- $\bar{y}_t^{i,j,m}$: aggregate flow from cell i to j at time t , i.e., $\bar{y}_t^{i,j} = \sum_{\forall p \in P} y_{p,t}^{i,j,m}, \forall (i, j) \in E; t \in T_f$,
- $\tilde{x}_t^{i,j}$: aggregate cell occupancy at diverging cell i at time t proceeding to cell j ,
- $r_{p,t}^m$: departure rate at time t for the flow using path p for user class m ,
- $TT_{p,t}$: travel time for the flow using path p at time t ,
- $\tau_{p,t,t'}$: auxiliary variable for maximum travel time estimation,
- $\hat{\tau}_{p,t,t'}$: auxiliary variable for maximum travel time estimation:
 $\hat{\tau}_{p,t,t'} = 1 - \tau_{p,t,t'}$,
- $\theta_{p,t,t'}$: auxiliary variable for maximum travel time estimation,
- $\nu_{p,t,t'}$: auxiliary variable for average travel time estimation.

An ordered pair of cells (i, j) represents a link and an ordered collection of links or an ordered collection of cells represents a path (similar to (Ukkusuri et al. 2012)). Also, a cell $i \in p$ implies that path p must contain cell i and a link $(i, j) \in p$ implies that path p must go through link (i, j) .

(b) Initialization:

At the beginning of the simulation ($t = 0$), the cell occupancies are set to zero for all paths and for all user classes in the network.

$$x_{p,0}^{i,m} = 0, \quad \forall i \in C, p \in P, m \in M; \tag{20}$$

$$y_{p,0}^{i,j,m} = 0, \quad \forall (i, j) \in E, p \in P, m \in M. \tag{21}$$

Source cells (C_R):

During network loading vehicles get into the source cells according to the demand pattern $r_{p,t}^m$. Based on the capacity (in and outflow rate), vehicles move to the next cell. For each path $p \in P$ containing source cells $i \in C_R$, the occupancy updates can be expressed as:

$$x_{p,t}^{i,m} = r_{p,t-1}^m + x_{p,t-1}^{i,m} - y_{p,t-1}^{i,j,m}, \quad \forall j \in \Gamma_i, t = \{1, \dots, t_e + 1\}, m \in M, \tag{22}$$

$$x_{p,t}^{i,m} = x_{p,t-1}^{i,m} - y_{p,t-1}^{i,j,m}, \quad \forall j \in \Gamma_i, t = \{t_e + 2, \dots, t_f\}, m \in M. \tag{23}$$

Now, each O-D pair has unique demand values for each user class $m \in M$ of the network. The cumulative departure rate should be equal to the total demand for a OD pair.

$$\sum_{p \in P^w} \sum_{t=0}^{t_e} r_{p,t}^m = d_w^m, \quad \forall w \in W, m \in M; \tag{24}$$

$$\sum_{m \in M} d_w^m = d_w, \quad \forall w \in W. \tag{25}$$

Ordinary cells (C_O):

An Ordinary cell, $i \in C_O$ has one incoming link and one outgoing link. The following equation updates the cell occupancy of an ordinary cell for a user class $m \in M$:

$$x_{p,t}^{i,m} = x_{p,t-1}^{i,m} + y_{p,t-1}^{k,i,m} - y_{p,t-1}^{i,j,m}, \quad \forall p \ni i, k \in \Gamma_i^{-1}, j \in \Gamma_i, t = \{1, \dots, t_f\}. \tag{26}$$

Also, if i not part of path p , then $x_{p,t}^{i,m} = 0$.

Diverging-merging cells (C_D):

The occupancy of any diverging and merging cell, $i \in C_D \cup C_M$ for a user class, $m \in M$ is updated updated as follows:

$$x_{p,t}^{i,m} = x_{p,t-1}^{i,m} + \sum_{k \in \Gamma_i^{-1}} y_{p,t-1}^{k,i,m} - \sum_{j \in \Gamma_i} y_{p,t-1}^{i,j,m}, \quad \forall p \ni k, i, j; k \in \Gamma_i^{-1}; j \in \Gamma_i; t = \{1, \dots, t_f\}. \tag{27}$$

Sink cells (C_S):

A sink cell $i \in C_S$ has limited in-flow capacity Q^i , however the storage capacity is unlimited ($N^i \rightarrow \infty$). The cell occupancy $x_{p,t}^{i,m}$ equals with the cumulative arrivals of path p in the period from 0 to t for user class $m \in \mathbb{M}$.

$$x_{p,t}^{i,m} = x_{p,t-1}^{i,m} + y_{p,t-1}^{k,i,m}, \quad \forall i \in C_S; p \ni i; k \in \Gamma_i^{-1}; t = \{1, \dots, t_f\}. \tag{28}$$

Ordinary links (E_O):

At the aggregate flow level, we have:

$$\bar{y}_t^{i,j} = \min(\bar{x}_t^i, Q^i, Q^j, \delta(N^j - \bar{x}_t^j)) \quad \forall (i, j) \in E_O; t = \{1, \dots, t_f\} \tag{29}$$

At the disaggregate level, we use the proportion of path-based cell occupancy $x_{p,t}^{i,m}$ and aggregate cell occupancy \bar{x}_t^i to determine the path flow $y_{p,t}^{i,j,m}$

$$y_{p,t}^{i,j,m} = \min(\bar{x}_t^i, Q^i, Q^j, \delta(N^j - \bar{x}_t^j)) \times \frac{x_{p,t}^{i,m}}{\bar{x}_t^i + \varsigma} \quad \forall (i, j) \in E_O; p \ni i; j \in \Gamma_i; t = \{1, \dots, t_f\} \tag{30}$$

Here $\varsigma > 0$ is an infinitesimal number used to make sure that the denominator is different from 0.

Diverging links (E_D):

The updates are similar to Ukkusuri et al. (2012) and aggregate occupancies are computed as follows:

$$\bar{x}_t^{i,j} = \sum_{\forall p \ni (i,j), m \in M} x_{p,t}^{i,m} \quad \forall i \in C_D; j \in \Gamma_i; t = \{1, \dots, t_f\} \tag{31}$$

$$\bar{x}_t^i = \sum_{j \in \Gamma_i} \bar{x}_t^{i,j} \quad \forall i \in C_D; t \in \{1, \dots, t_f\}, \tag{32}$$

For the diverging flows:

For all $i \in C_D; j \in \Gamma_i; t = \{1, \dots, t_f\}$,

$$\bar{y}_t^{i,j} = \min(\bar{x}_t^{i,j}, Q^j, \delta(N^j - \bar{x}_t^j)) \times \min\left(1, \frac{Q^i}{\sum_{j' \in \Gamma_i} (\min(\bar{x}_t^{i,j'}, Q^{j'}, \delta(N^{j'} - \bar{x}_t^{j'}))) + \mu}\right) \tag{33}$$

Ukkusuri et al. (2012) use the proportional rule to obtain the flow for each path from each O-D pair:

$$y_{p,t}^{i,j,m} = \bar{y}_t^{i,j} \times \frac{x_{p,t}^{i,m}}{\bar{x}_t^{i,j} + \varsigma} \quad \forall i \in C_D; p \ni i; j \in \Gamma_i; t \in \{1, \dots, t_f\} \tag{34}$$

Merging links (E_D):

The updating for merging links are computed by the following equations:

For all $i \in C_M; k \in \Gamma_i^{-1}; t = \{1, \dots, t_f\}$,

$$\bar{y}_t^{k,i} = \min(Q^k, \bar{x}_t^k) \times \min\left(1, \frac{\min(Q^i, \delta(N^i - \bar{x}_t^i))}{\sum_{k' \in \Gamma_i^{-1}} (\min(Q^{k'}, \bar{x}_t^{k'})) + \varsigma}\right). \tag{35}$$

The flow for each path of each O-D pair can be computed as:

$$y_{p,t}^{k,i,m} = \bar{y}_t^{k,i} \times \frac{x_{p,t}^{k,m}}{\bar{x}_t^k + \varsigma} \quad \forall i \in C_M; p \ni i; k \in \Gamma_i^{-1}; t \in \{1, \dots, t_f\} \tag{36}$$

Appendix B: Travel time estimation using CTM

Ramadurai (2009) and Han et al. (2011) provide details on computing average travel time within the path-based CTM model. For the completeness of our discussion we mention the equations from Ukkusuri et al. (2012).

$$v_{p,t,t'} = \max\left(0, \sum_{h=0}^t r_{p,h} - x_{p,t'}^s\right), \tag{37}$$

$\forall p \in P; s \in p \cap C_S; t = \{0, \dots, t_e\}; t' = \{t, \dots, t_f\}$

$$TT_{p,0} = \frac{\sum_{h=0}^{T_f-1} (v_{p,0,h} - v_{p,0,h+1})h}{r_{p,0} + \mu}, \forall p \in P \tag{38}$$

$$TT_{p,t} = \frac{\sum_{h=t}^{T_f-1} (v_{p,t,h} - v_{p,t,h+1} + v_{p,t-1,h+1} - v_{p,t-1,h})(h-t)}{r_{p,t} + \mu}, \tag{39}$$

$\forall p \in P; s \in p \cap C_S; t = 0, \dots, T.$

Users from all classes experience the same travel time. Therefore, the average travel time computation is not specific for a class.

$$r_{p,h} = \sum_{m \in M} r_{p,t}^m, \tag{40}$$

$$x_{p,t'}^s = \sum_{m \in M} x_{p,t'}^{s,m}. \tag{41}$$

Now, the max operator can be replaced by the following complementarity conditions:

$$0 \leq v_{p,t,t'} \perp v_{p,t,t'} - \left(\sum_{h=0}^t r_{p,h} - x_{p,t'}^s\right) \geq 0$$

$\forall p \in P; t = \{0, \dots, t_e\}; t' = \{t, \dots, t_f\}.$ (42)

Algorithm step (Zhan and Ukkusuri 2014)

Step 0: Set counter $k=0$. Initialize a feasible departure rate.

Step 1: Run the simulation $CTM(\gamma^k)$ and compute $TC(\gamma^k)$, $CC(\gamma^k)$, $GC(\gamma^k)$.

Step 2: Decompose $\gamma^k = (\gamma_1^k, \gamma_2^k, \dots, \gamma_m^k)^T$.

Step 3: Find the $\lambda^k(\gamma^k)$ that ensures most number of user classes and OD pairs satisfy: $\|T_i(\gamma_i^k) - T_i(\gamma_i^{k-1})\| \leq \alpha \|\gamma_i^k - \gamma_i^{k-1}\|$, in which $T_i(\gamma_i^k) = Pr_{\Omega_i}[\gamma_i^k - \lambda^k(\gamma^k)GC_i(\gamma^k)]$

Step 4: Update departure rate γ_i^k using mapping T_i only for those user classes and OD pairs that satisfy the condition in Step 3. For others that not satisfied, set $\gamma_j^k = \gamma_j^{k-1}$.

Step 5: If none of the user classes and OD pairs are found satisfy condition in Step 3, set $\gamma_j^k = \gamma_j^{k-1}$, $\lambda^k(\gamma^k) = \lambda^{k-1}(\gamma^{k-1})/2$.

Step 6: If $\|z^* - \gamma^k\| \leq \epsilon$, terminate the algorithm, $\gamma^* = z^*$. Otherwise $\gamma^{k+1} = \gamma^k$, Set $k = k + 1$, go to step 1.

Appendix C: DUE Results

C.1. DUE-1 with base case: Sioux-Falls

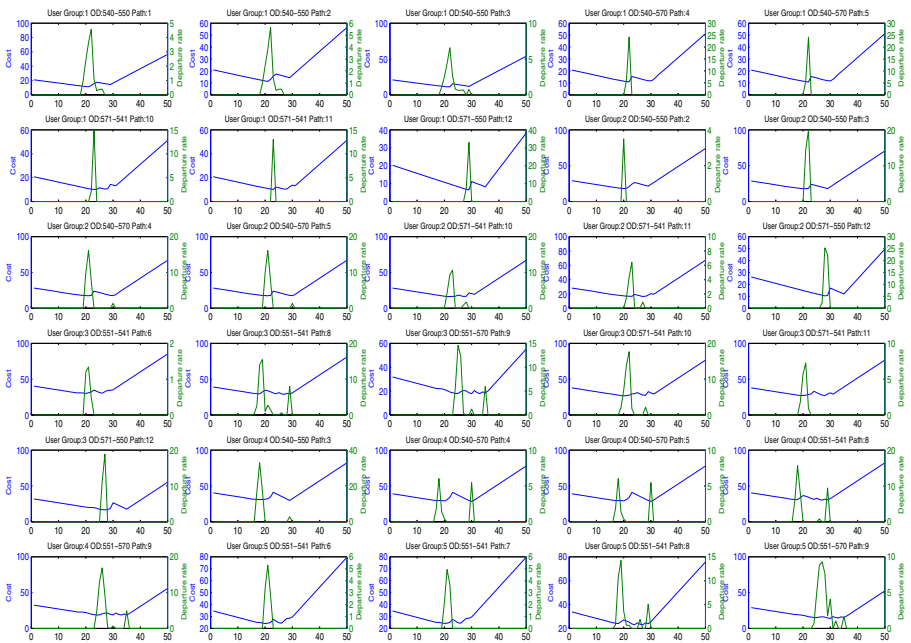


Fig. 17 PMCA-DUE-1 results base case: no carbon cap

C.2. DUE-2 with 2 % reduction: Sioux-Falls

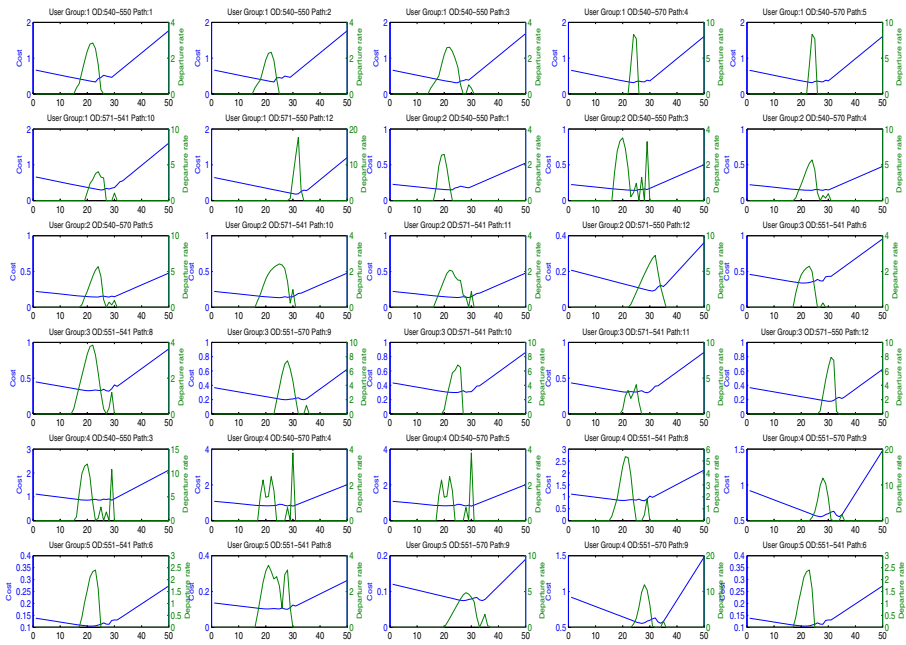


Fig. 18 PMCA-DUE-2 results: 2 % reduction from base case

C.3. DUE-3 with 2 % reduction: Sioux-Falls

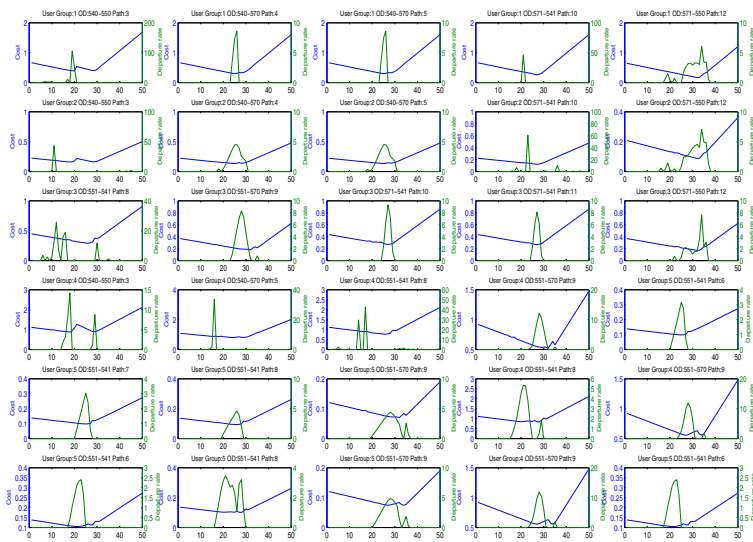


Fig. 19 PMCA-DUE-3 results: 2 % reduction from base case

References

- Ahn K, Rakha H (2008) The effects of route choice decisions on vehicle energy consumption and emissions. *Transp Res Part D: Transp Environ* 13(3):151–167
- Ahn K, Rakha H, Trani A, Van Aerde M (2002) Estimating vehicle fuel consumption and emissions based on instantaneous speed and acceleration levels. *J Transp Eng* 128(2):182–190
- Aziz HMA (2014) Integrating pro-environmental behavior with transportation network modeling: User and system level strategies, implementation, and evaluation. Doctoral dissertation, Purdue University, West Lafayette, Indiana, USA
- Aziz HMA, Ukkusuri S (2013) Tradable emissions credits for personal travel: a market-based approach to achieve air quality standards. *Int J Adv Eng Sci Appl Math* 5(2-3):145–157
- Aziz HMA, Ukkusuri SV (2012) Integration of environmental objectives in a system optimal dynamic traffic assignment model. *Comput-Aided Civ Infrastruct Eng* 27(7):494–511
- Aziz HMA, Ukkusuri SV, Romero J (2015) Understanding short-term travel behavior under personal mobility credit allowance scheme using experimental economics. *Transp Res Part D: Transp Environ* 36:121–137
- Barth M, Boriboonsomsin K (2008) Real-world carbon dioxide impacts of traffic congestion. *Transp Res Record: J Transp Res Board* 2058:163–171
- Barth M, Scora G, Younglove T (2004) Modal emissions model for heavy-duty diesel vehicles. *Transp Res Record: J Transp Res Board* 1880:10–20
- Bottrill C (2006) Understanding dtqs and pcas. Environmental Change Institute/UKERC Working Paper
- Bristow AL, Wardman M, Zanni AM, Chintakayala PK (2010) Public acceptability of personal carbon trading and carbon tax. *Ecol Econ* 69(9):1824–1837
- Burtraw D (2002) Markets for clean air: the u.s. acid rain program: A. denny ellerman, paul i. joskow, richard schmalensee, juan-pablo montero, elizabeth m. bailey, cambridge, uk: Cambridge university press, 2000. *Reg Sci Urban Econ* 32(1):139–144
- Capstick SB, Lewis A (2010) Effects of personal carbon allowances on decision-making: evidence from an experimental simulation. *Clim Pol* 10(4):369–384
- Carey M, Balijepalli C, Watling D (2015) Extending the cell transmission model to multiple lanes and lane-changing. *Networks and Spatial Economics* 15(3):507–535
- Chen L, Yang H (2012) Managing congestion and emissions in road networks with tolls and rebates. *Transp Res B Methodol* 46(8):933–948
- Coase RH (1960) The problem of social cost. *Journal of Law and Economics* 3 (ArticleType: research-article / Full publication date: Oct., 1960 / Copyright 1960 The University of Chicago)
- Connection TLE (2009) Defra's pre-feasibility study into personal carbon trading-a missed opportunity
- Daganzo CF (1994) The cell transmission model: a simple dynamic representation of highway traffic. *Transp Res B* 28(4):269–287
- Daganzo CF (1995) The cell transmission model, part ii: Network traffic. *Transp Res B* 29(2):79–93
- Dales J (1968) Pollution, property, and prices. University of Toronto Press, Toronto
- DEFRA (2008) Synthesis report on the findings from defras pre-feasibility study into personal carbon trading. Department of Environment Food, and Rural Affairs
- Dresner S, Ekins P (2004) The distributional impacts of economic instruments to limit greenhouse gas emissions from transport. Policy Studies Institute, UK
- DTA (2011) Dynamic traffic assignment: A primer. *Transp Res Circular Report:C153*
- EIA (2014) Annual Energy Outlook (2014) US Energy Information Administration. US Department of Energy, Washington
- Eyre N (2010) Policing carbon: design and enforcement options for personal carbon trading. *Clim Pol* 10(4):432–446
- Fawcett T (2010) Personal carbon trading: A policy ahead of its time *Energy Policy* 38(11):6868–6876
- Fawcett T (2012) Personal carbon trading: is now the right time *Carbon Manage* 3(3):283–291
- Fawcett T, Parag Y (2010) An introduction to personal carbon trading. *Clim Pol* 10(4):329–338
- Fleming D (1997) Tradable quotas: using information technology to cap national carbon emissions. *Eur Environ* 7(5):139–148
- Fleming D, Chamberlin S (2011) Teqs(tradable energy quotas): A policy framework for peak oil and climate change. London: All-Party Parliamentary Group on Peak Oil, and The Lean Economy Connection

- Gardner LM, Duell M, Waller ST (2013) A framework for evaluating the role of electric vehicles in transportation network infrastructure under travel demand variability. *Transp Res A Policy Pract* 49(0):76–90
- Grayling T, Gibbs T (2006) Tailpipe trading: how to include road transport in the eu emissions trading scheme (eu ets). Institute for Public Policy Research, LowCVP Low Carbon Road Transport Challenge
- Han L, Ukkusuri S, Doan K (2011) Complementarity formulations for the cell transmission model based dynamic user equilibrium with departure time choice, elastic demand and user heterogeneity. *Transp Res B Methodol* 45(10):1749–1767
- Harwatt H, Tight M, Bristow AL, Guhnemann A (2011) Personal carbon trading and fuel price increases in the transport sector: an exploratory study of public response in the uk. *European Transport Trasporti Europei* 47:47–70
- Hearn DW, Ramana MV (1998) Solving congestion toll pricing models. In: Marcotte NSP (ed) *Equilibrium and Advanced Transportation Modeling.*, Kluwer Academic Publishers, Norwell
- Hillman M, Fawcett T (2008) Rajan SC. St Martin's Griffin, How we can save the planet: Preventing global climate catastrophe
- Howell RA (2012) Living with a carbon allowance: The experiences of carbon rationing action groups and implications for policy. *Energy Policy* 41(0):250–258
- Keay-Bright S, Fawcett T (2005) Taxing and trading: Debating options for carbon reduction, UK Energy Research Centre Meeting Report
- Keppens M, Vereeck L (2003) The design and effects of a tradable fuel permit system. In: *PROCEEDINGS OF THE EUROPEAN TRANSPORT CONFERENCE (ETC) 2003 HELD 8-10 OCTOBER 2003, STRASBOURG, FRANCE*
- Kitthamkesorn S, Chen A, Xu X, Ryu S (2016) Modeling mode and route similarities in network equilibrium problem with go-green modes. *Netw Spatial Econ* 16(1):33–60
- Kockelman KM, Kalmanje S (2005) Credit-based congestion pricing: a policy proposal and the publics response. *Transp Res A Policy Pract* 39(79):671–690
- Lin J, Chen Q, Kawamura K (2016a) Sustainability si: logistics cost and environmental impact analyses of urban delivery consolidation strategies. *Netw Spatial Econ* 16(1):227–253
- Lin X, Tampère CM, Viti F, Immers B (2016b) The cost of environmental constraints in traffic networks: assessing the loss of optimality. *Netw Spatial Econ* 16(1):349–369
- Ma R, Ban X, Pang JS, Liu HX (2015) Submission to the dta2012 special issue: Approximating time delays in solving continuous-time dynamic user equilibria. *Netw Spatial Econ* 15(3):443–463. Jeff
- Mascia M, Hu S, Han K, North R, Poppel M, Theunis J, Beckx C, Litzzenberger M (2016) Impact of traffic management on black carbon emissions: a microsimulation study. *Netw Spatial Econ*:1–23
- Merchant DK, Nemhauser GL (1978) A model and an algorithm for the dynamic traffic assignment problems. *Transplant Sci* 12(3):183–199
- Montgomery WD (1972) Markets in licenses and efficient pollution control programs. *J Econ Theory* 5(3):395–418
- Nagurney A, Zhang D (2001) Dynamics of a transportation pollution permit system with stability analysis and computations. *Transp Res Part D: Transp Environ* 6(4):243–268
- Nezamuddin N, Boyles SD (2015) A continuous due algorithm using the link transmission model. *Netw Spatial Econ* 15(3):465–483
- Nie Y (2012) Transaction costs and tradable mobility credits. *Transp Res B Methodol* 46(1):189–203
- Nie Y, Yin Y (2013) Managing rush hour travel choices with tradable credit scheme. *Transp Res B Methodol* 50(0):1–19
- Niemeier D, Gould G, Karner A, Hixson M, Bachmann B, Okma C, Lang Z, Heres Del Valle D (2008) Rethinking downstream regulation: California's opportunity to engage households in reducing greenhouse gases. *Energy Policy* 36(9):3436–3447
- Parag Y, Strickland D (2010) Personal carbon trading: A radical policy option for reducing emissions from the domestic sector. *Environ Sci Policy for Sustainable Dev* 53(1):29–37
- Perrels A (2010) User response and equity considerations regarding emission cap-and-trade schemes for travel. *Energy Effic* 3(2):149–165
- Ramadurai G (2009) Novel dynamic user equilibrium models: analytical formulations, multi-dimensional choice, and an efficient algorithm. PhD thesis, Department of civil and environmental engineering, Rensselaer Polytechnic Institute (Troy, NY)
- Ramadurai G, Ukkusuri S (2007) Dynamic traffic equilibrium: Theoretical and experimental network game results in single-bottleneck model. *Transp Res Record: J Trans Res Board* 2029:1–13

- Raux C, Marlot G (2005) A system of tradable co2 permits applied to fuel consumption by motorists. *Transp Policy* 12(3):255–265
- Roberts S, Thumim J (2006) A rough guide to individual carbon trading: The ideas, the issues and the next steps, report to defra
- Sloboden J, Alexiadis V, Chiu YC, Nava E (2012) Traffic analysis toolbox volume xiv: Guidebook on the utilization of dynamic traffic assignment in modeling. US Department of Transportation Federal Highway Administration FHWA-HOP-13-015
- Starkey R (2008) Allocating emissions rights: Are equal shares, fair shares. Tyndall Centre for Climate Change Research, Manchester
- Starkey R (2012a) Personal carbon trading: A critical survey: Part 1: Equity. *Ecol Econ* 73(0):7–18
- Starkey R (2012b) Personal carbon trading: A critical survey part 2: Efficiency and effectiveness. *Ecol Econ* 73(0):19–28
- Starkey R, Anderson K (2005) Domestic tradable quotas: A policy instrument for reducing greenhouse gas emissions from energy use. Tyndall Centre for Climate Change Research Norwich, UK
- Szeto WY (2013) Cell-based dynamic equilibrium models. *Adv Dyn Netw Model Complex Transp Syst* 2:163–192
- Thumim J, White V (2008) Distributional impacts of personal carbon trading: A report to the department for environment, food and rural affairs. Centre for Sust Energ:1
- Tietenberg T (2003) The tradable-permits approach to protecting the commons: Lessons for climate change. *Oxf Rev Econ Policy* 19(3):400–419
- Ukkusuri SV, Han L, Doan K (2012) Dynamic user equilibrium with a path based cell transmission model for general traffic networks. *Transp Res B Methodol* 46(10):1657–1684
- US DOT R (2011) The value of travel time savings: Departmental guidance for conducting economic evaluations (revision 2). US Department of Transportation (<http://ostpxwebdotgov/policy/reportshtm>)
- Verhoef E, Nijkamp P, Rietveld P (1997) Tradeable permits: their potential in the regulation of road transport externalities. *Environ Planning B: Planning and Des* 24(4):527–548
- Verhoef ET, Small KA (2004) Product differentiation on roads: constrained congestion pricing with heterogeneous users. *J Transp Econ Policy* 38(1):127–156
- Wadud Z (2011) Personal tradable carbon permits for road transport: Why, why not and who wins *Transp Res A Policy Pract* 45(10):1052–1065
- Yang H, Bell MG (1998) Models and algorithms for road network design: a review and some new developments. *Transp Rev A transnat Transdisciplinary J* 18(3):257–278
- Yang H, Huang HJ (2004) The multi-class, multi-criteria traffic network equilibrium and systems optimum problem. *Transp Res B Methodol* 38(1):1–15
- Yang H, Wang X (2011) Managing network mobility with tradable credits. *Transp Res B Methodol* 45(3):580–594
- Yin Y, Lawphongpanich S (2006) Internalizing emission externality on road networks. *Transp Res Part D: Transp Environ* 11(4):292–301
- Zhan X, Ukkusuri SV (2014) Multi-user class, simultaneous route and departure time choice dynamic traffic assignment with an embedded spatial queuing model. 5th International Symposium on Dynamic Traffic Assignment Salerno:Italy
- Ziliaskopoulos AK (2000) A linear programming model for the single destination system optimum dynamic traffic assignment problem. *Transp Sci* 34(1):37–49